Diplomarbeit

The effects of the pan HDAC inhibitor Vorinostat on contractility and calcium cycling in murine ventricular cardiomyocytes

eingereicht von

Michael Simon Kasa

zur Erlangung des akademischen Grades

Doktor(in) der gesamten Heilkunde

(Dr. med. univ.)

an der

Medizinischen Universität Graz

ausgeführt am

Universitätsklinikum für Innere Medizin

Klinische Abteilung für Kardiologie

unter der Anleitung von

Assoz. Prof. Priv.-Doz. Dr.med.univ. Dr.scient.med. Peter Rainer

Priv.-Doz. Dr.med.univ. Dr.scient.med. Markus Wallner

Graz, 03.03.2021

Eidesstattliche Erklärung

Ich erkläre ehrenwörtlich, dass ich die vorliegende Arbeit selbstständig und ohne fremde Hilfe verfasst habe, andere als die angegebenen Quellen nicht verwendet habe und die den benutzten Quellen wörtlich oder inhaltlich entnommenen Stellen als solche kenntlich gemacht habe.

Graz, am 03.03.2021 *Michael Simon Kasa eh.*

Vorwort

Diese Arbeit will ich einer speziellen Person widmen, Alexander Krois. Er war nicht nur ein guter Freund und Studienkollege für mich, er war es auch, der mich mit der klinischen Abteilung für Kardiologie in Verbindung gebracht hat. Tragischerweise wurde er viel zu früh aus seinem Leben gerissen, in Gedanken wird er immer präsent bleiben.

Zu besonderen Dank bin ich allen Kolleginnen und Kollegen verpflichtet, die am Gelingen dieser Arbeit beteiligt waren und von denen ich mittlerweile viele auch zu meinen Freunden zählen darf. Insbesondere zwei Personen will ich hervorheben: Chintan Koyani, welcher mir mit viel Erfahrung und Wissen beiseite Stand und mir vor allem bei der Isolation der Cardiomyocyten maßgeblich geholfen hat und Deborah M. Eaton, welche mir bei der Inkubation und Fehlersuche wegweisende Ratschläge erteilt hat.

Ein herzliches „Dankeschön!“ gebührt meinen beiden Diplomarbeitsbetreuern, Markus Wallner und Peter Rainer. Beide unterstützten mich großzügig und standen stets mit Rat und Tat zur Seite. Der vertrauensvolle Führungsstil ermöglichte es mir, in der Zeit enorm viel zu lernen und mich persönlich zu entfalten. Weiters wurden mir auch Chancen eröffnet, mich an weiteren Projekten zu beteiligen.

Zu guter Letzt aber gilt meine besondere Dankbarkeit meiner Familie, die mir das Studium ermöglicht hat und mir jedwede Unterstützung zukommen ließ.

Table of content

List of abbreviations

6MWD	6-min walk distance
2,3 - BDM	2,3-Butanedione monoxime
ACEi	Angiotensin-converting enzyme inhibitors
AF	Atrial fibrillation
AHA	American Heart Association
aHT	Arterial Hypertension
AM	Acetoxymethyl
ASD	Atrial septal defect
ATP	Adenosine triphosphate
BCS	Bovine calf serum
bl	Baseline
BMI	Body mass index
BMI	Body mass index
BNP	Brain natriuretic peptide
BSA	Bovine serum albumin
CAD	Coronary artery disease
CaMK	Ca2+/calmodulin-dependent protein kinase
CHO	Chinese hamster ovaries
CM	Cardiomyocyte
CO	Cardiac output
COPD	Chronic obstructive pulmonary disease
CRP	C-reactive protein
CV	Cardio-vascular
DAD	Deacetylase activating domain
DD	Diastolic dysfunction
DHPR	Dihydropyridine receptors
DM	Diabetes mellitus
DMSO	Dimethylsulfoxid
ECG	Electrocardiography
ECM	Extracellular Matrix
ED	Endothelial Dysfunction
EDP	End-diastolic pressure
EDV	End-diastolic volume

EF	Ejection fraction
ESC	European Society of Cardiology
HAT	Histone acetyl tranferase
HDAC	Histone-Deacetylases
HDACi	Histone-Deacetylases inhibitors
HF	Heart failure
HFmrEF	Heart failure with mid-range ejection fraction
HFpEF	Heart failure with preserved ejection fraction
HFrEF	Heart failure with reduced ejection fraction
HHD	Hypertensive heart disease
HPRT	Hypoxanthin-Phosphoribosyl-Transferase
hsCRP	high-sensitivity C-reactive protein
hsTNT	High sensitivity Troponin T
IASD	Interatrial shunt device
Ig	Immunoglobulin
Il - [...]	Interleukin [e.g. 1, 6, …]
Iso	Isoproterenol ≙ Isoprenaline
LA	Left atrium
LAP	Left atrial pressure
LS	Longitudinal strain
LVEDP	Left ventricular end-diastolic pressure
LVEF	Left ventricular ejection fraction
MAGGIC	Meta-analysis Global Group in Chronic Heart Failure
MDS	Myocyte Digestion Solution
MEF2	Myocyte enhancer factor-2
MI	Myocardial infarction
MLWHF	Minnesota Living with Heart Failure Score
MMP-1	Matrix metalloproteinase - 1
mPAP	mean Pulmonary artery pressure
MRA	Mineralocorticoid receptor antagonists
mRNA	Messenger Ribonucleic acid
MRS	Magnetic resonance spectroscopy
MSS	Myocyte Stopping Solution
MVD	Microvascular depletion

MyHC	Myosin heavy chain
N-CoR	Nuclear receptor co-repressor
NCX	Na+/Ca2+ exchanger
NO	Nitric Oxide
NP	Natriuretic peptide
NT	Normal Tyrode
NT-proBNP	N-terminal prohormone of brain natriuretic peptide
NYHA	New York Heart Association
PB	Perfusion Buffer
PCr	Creatine phosphate
PCWP	Pulmonary capillary wedge pressure
PKA	Protein kinase A
PMCA	Plasma membrane Ca2+ ATPase
PMT	Photo multiplier tube
RAAS	Renin Angiotensin Aldosterone system
ROS	Reactive oxygen species
RVEF	Right ventricular ejection fraction
RyR2	Ryanodine receptor 2
SAHA	Suberoylanilide hydroxamic acid ≙ Vorinostat
SERCA	Sarcoplasmic/endoplasmic reticulum Ca2+-ATPase pump
SMRT	Silencing mediator for retinoid acid and thyroid receptors
SR	Sarcoplasmic reticulum
SV	Stroke volume
TEE	Transoesophageal echocardiography
TGF-β	Transforming growth factor β
TIMP-1	Tissue inhibitor of metalloproteinases - 1
TNF-α	Tumor necrosis factor α
TSA	Trichostatin A
TTE	Transthoracic echocardiography
t-tubule	Transverse tubule
WBC	White blood cell

Table of figures

List of tables

Zusammenfassung

Einleitung

Herzinsuffizienz mit einer erhaltenen systolischen Pumpfunktion (HFpEF) stellt bereits heute ein signifikantes Gesundheitsproblem dar, wobei die Prävalenz im Verlauf der nächsten Jahrzehnte zunehmen soll. Frauen und ältere Patientinnen bzw. Patienten sind von der Erkrankung statistisch häufiger betroffen. Derzeit existiert keine effektive medikamentöse Therapie, jedoch konnte in rezenter Literatur in präklinischen Versuchen ein positiver Effekt auf die systolische und diastolische Herzfunktion durch die Behandlung mit Histon-Deacetylasen-Inhibitoren (HDACi) gezeigt werden. Diese Wirkstoffgruppe führt zu einer verstärkten Acetylierung verschiedener Proteine, jedoch ist der kausale Wirkungsmechanismus bei HFpEF derzeit nur unzureichend verstanden. Ziel der Studie war es, den Effekt des HDACi Suberanilohydroxamic Acid (SAHA) auf die Kontraktilität und den Calciumstoffwechsel in ventrikulären Herzmuskelzellen (Cardiomyocytes, CM) von Mäusen zu untersuchen.

Methoden

Für die Messungen wurden aus C57BL/6J – Mäusen (n=5) ventrikuläre CM isoliert. Diese Zellen (n=32) wurden anschließend für 90 Minuten mit 5 µM SAHA inkubiert. Die Kontraktilität des Sarkomers sowie das zytosolische Calcium wurden an elektrisch stimulierten CM mit Hilfe eines Epifluoreszenz Mikroskops bestimmt und mit unbehandelten Zellen (n=30) verglichen.

Resultate

Die Behandlung mit SAHA hat weder bei baseline Bedingungen noch bei maximaler β-mimetischer Stimulation mit Isoproterenol zu Veränderungen der diastolischen Sarkomerlänge, -verkürzungsamplitude oder Relaxation der Zellen geführt. Diastolisches Calcium, -Amplitude sowie die Relaxationsparameter RT10 und RT50 waren in beiden Gruppen vergleichbar.

Fazit

In der Zusammenschau verfügbarer Literatur zeigt eine Behandlung von Ratten (in-vitro) und Katzen (in-vivo) mit pan-HDACi SAHA signifikante Verbesserungen sowohl der systolischen, als auch der diastolischen Herzfunktion. In den im Rahmen dieser Arbeit durchgeführten Experimenten konnte durch eine akute Behandlung von murinen CM mit SAHA weder auf die Sarkomer-Kinetik noch auf den Kalzium-Stoffwechsel der Zellen eine signifikante Veränderung der untersuchten Parameter festgestellt werden.

Abstract

Introduction

Heart failure (HF) with preserved ejection fraction (HFpEF) is an increasing worldwide health problem with no proven effective therapies, disproportionately affecting women and the elderly. It was previously shown that inhibition of histone deacytelase catalytic activity improves cardiac systolic and diastolic function in rodent and feline models of HFpEF via hyperacetylation of a variety of proteins. The specific mechanisms underlying enhanced cardiac function are not fully understood. The aim of this study was to assess the effects of suberanilohydroxamic acid (SAHA), a pan-HDAC inhibitor, on calcium cycling and sarcomere kinetics in murine ventricular cardiomyocytes.

Methods

Experiments were performed using ventricular cardiomyocytes (CM) isolated from healthy C57BL/6J mice (n=5). Freshly isolated murine CM were incubated with 5 μM SAHA (n=32) for 90 minutes and compared to vehicle treated CM (n=30). Sarcomere shortening and cytosolic calcium were measured using an epifluorescence microscope and calcium sensitive dyes while the cells were electrically stimulated.

Results

SAHA did not induce any changes in diastolic sarcomere length, shortening amplitude, or parameters of relaxation in murine CM, both at baseline and following exposure to the β - adrenergic agonist Isoproterenol. Furthermore, diastolic calcium levels, amplitude as well as RT10 and RT50 were unaffected by SAHA.

Conclusions

Current literature contains substantial evidence that SAHA treatment results in a significant improvement in both contraction and relaxation characteristics of feline (in-vivo) and rat (in vitro) CM. However, with the experiments conducted for this thesis, we were not able to detect any significant effect elicited by the short-term incubation of murine ventricular CM with the panHDACi Vorinostat.

1 Introduction

1.1 CV disease in Austria

In Austria, the leading cause of death are cardio-vascular (CV) diseases, being responsible for 39% of all deaths in 2018. Although the relative proportion declined from 53% in 1988, it remains high. *(see Figure 1)* Therefore, there is great interest, both from the industry, as well as the national health service, in developing better therapies to reduce morbidity and mortality. (1)

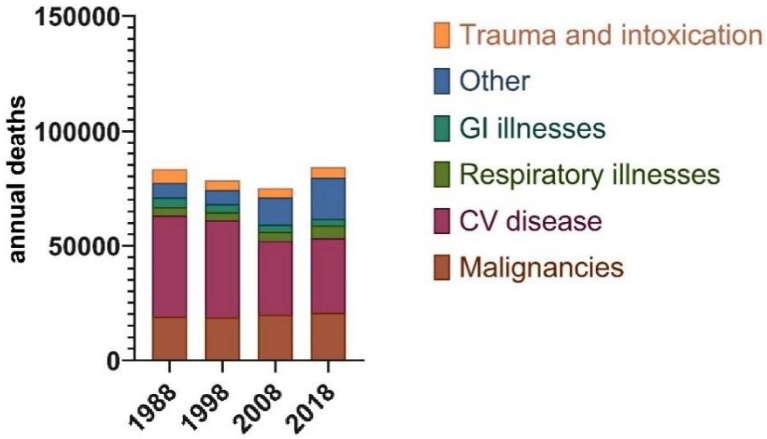

Figure 1 All-cause mortality in Austria in the years 1988 – 2018

*modified after **(1)**, Data © Statistik Austria*

CV illnesses cover a heterogeneous group of diseases, ranging from stroke to myocardial infarction. In this group the leading reason for mortality, acute myocardial infarction, decreased due to better available therapies (e.g. PTCA and better prehospital treatment), as well as prevention, from 21% in 1988 to 14% in 2018, though the incidence stayed roughly the same. (2)

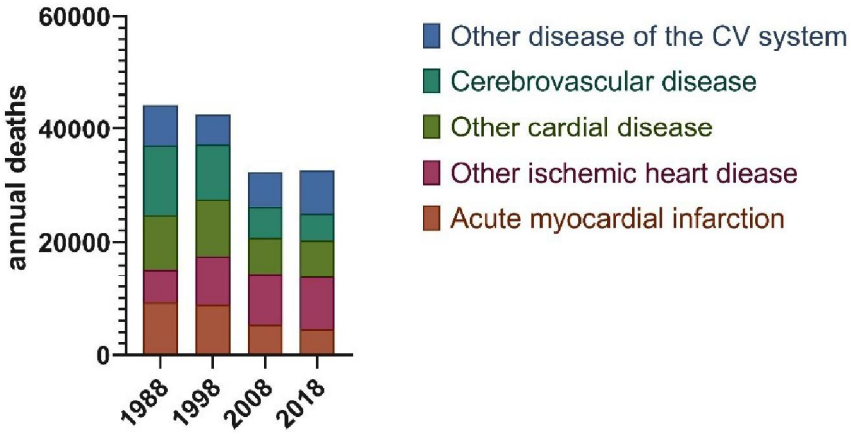

Table 1 Cardio-vascular (CV) related deaths in Austria in the years 1988 – 2018

*modified after**(2)**, Data © Statistik Austria*

Though during the same period, another sub-group became more prevalent, other ischemic heart diseases are now the leading cause of death. Their relative percentage increased from 14% in 1988 to 28% in 2018. This may be partially due to the better acute treatment, so patients survive to develop the later stages of disease and/or due to other diseases developing, as a result of wealth related illnesses (e.g. diabetes mellitus and hypertension). Other, non-ischemic, heart diseases remain relatively unchanged over the course of the last 30 years, causing 20% of CV related deaths.

At the beginning of most cardio-vascular pathologies is a low-grade proinflammatory state, leading subsequently to atherosclerosis. Atherosclerosis, as it progresses over time, lays the groundwork for events like (myocardial-) infarction, stroke, or ischemic cardiomyopathies. Some of these (cardiac-) pathologies progress over time into a clinical syndrome called heart failure (*HF*).

1.2 Heart failure

The European Society of Cardiology (*ESC*) defines HF as:

> *"[…] a clinical syndrome characterized by typical symptoms (e.g. breathlessness, ankle swelling and fatigue) that may be accompanied by signs (e.g. elevated jugular venous pressure, pulmonary crackles and peripheral oedema) caused by a structural and/or functional cardiac abnormality, resulting in a reduced cardiac output and/or elevated intracardiac pressures at rest or during stress."*(3)

HF is a syndrome characterised by the clinical features of a decreased organ perfusion as well as increased tissue and organ fluid content. (4)

Due to that broad definition, heart failure covers a very heterogeneous clinical syndrome. The underlying aetiologies are vastly different and are influenced by the wealth of the region. In the United States of America, 60% of patients with heart failure suffer from coronary artery disease (*CAD*) and 70% from hypertension. In most African and Asian countries the driving causes are rheumatologic issues, high blood pressure and nutrient deficiencies. As these countries are developing, the lifestyle is becoming more and more alike the USA and Europe, also the diseases are converging. (5)

HF is a causing a substantial burden to private- and public health. It reduces the patient's quality of life significantly (6) and influences the allocation of a country's health care funds hugely. Annual costs in the US were estimated to reach $60.2 billion dollar in

2013 alone. (7) Worldwide HF due to pericardial, myocardial, endocardial and valvular injuries account for more than 5% of hospital admissions. (5)

1.2.1 Classification of HF

1.2.1.1 According to EF

Due to the heterogeneity of the disease, a useful phenotypic marker was needed to differentiate the varying underlying pathophysiological mechanisms. This could allow at best for well- defined subgroups, being better eligible for clinical trials, therapies, as well as more precise prognosis. In patients that were examined with echocardiography, a bimodal distribution of patients could be identified using the ejection fraction (*EF*).(8)(*see chapter 1.2.1.1.1*) Therefore EF was used to separate two distinct entities of the disease, heart failure with preserved ejection fraction (*HFpEF*) and heart failure with reduced ejection fraction (*HFrEF*). (*see Table 2*)

In the latest ESCs guidelines for heart failure of 2016 the authors defined the "grey area" in between these two groups – patients with an EF between 40% and 49% - as new subgroup, referring to them as "HF with mid-range EF (*HFmrEF*)". (3) (*see Table 2*)

Though in recent years there is increasing concern using this parameter as divider, since EF is a marker which is highly dependent on different patient related and non-patient related factors. Hence numerous authors argue, the EF is not truly able to represent the systolic function of the heart.(9,10) Despite the different drawbacks EF is still widely used, since this parameter was very well validated, in regards to therapy, prognosis in numerous trials. These trials lay the groundwork for today's guideline directed therapies. (*see below, chapter 1.2.1.1.1*)

Type of HF		HFrEF	HFmrEF	HFpEF
CRITERIA	1	Symptoms ± Signs[a]	Symptoms ± Signs[a]	Symptoms ± Signs[a]
	2	LVEF <40%	LVEF 40–49%	LVEF ≥50%
	3	–	1. Elevated levels of natriuretic peptides[b]; 2. At least one additional criterion: a. relevant structural heart disease (LVH and/or LAE), b. diastolic dysfunction (for details see Section 4.3.2).	1. Elevated levels of natriuretic peptides[b]; 2. At least one additional criterion: a. relevant structural heart disease (LVH and/or LAE), b. diastolic dysfunction (for details see Section 4.3.2).

BNP = B-type natriuretic peptide; HF = heart failure; HFmrEF = heart failure with mid-range ejection fraction; HFpEF = heart failure with preserved ejection fraction; HFrEF = heart failure with reduced ejection fraction; LAE = left atrial enlargement; LVEF = left ventricular ejection fraction; LVH = left ventricular hypertrophy; NT-proBNP = N-terminal pro-B type natriuretic peptide.
[a]Signs may not be present in the early stages of HF (especially in HFpEF) and in patients treated with diuretics.
[b]BNP>35 pg/ml and/or NT-proBNP>125 pg/mL.

Table 2 Diagnostic criteria for the different forms of HF according to ESCs latest definition(3)

©2016 ESC

1.2.1.1.1 Ejection fraction (EF)

The ejection fraction is defined as the ratio between the stroke volume (*SV*) and the ventricular end-diastolic volume (*EDV*). In clinical practice EF is the most used measurement to quantify the systolic function of chambers of the heart. EF can be measured for the right (*RVEF*) and the left ventricle (*LVEF*) as well as the atria. Measurements for the left ventricle are more common, hence the LVEF is mostly only referred as EF. The resulting number is noted in %. (11)

EF can be measured using different imaging modalities, though an echocardiographic quantification is the most used methodology. The fact that – in contrast to tomographic techniques – EF is only estimated with echocardiography, remains a particular challenge. Geometric assumptions are used to calculate a (3D-) volume based on 2D pictures. Therefore, EF is prone to various confounders, for example the loading-conditions, geometry of the ventricle or the observers themselves. (9) Furthermore, as delineated above, EF is a mere ratio of volumes and therefore rather an indicator of LV capacitance and remodelling than a measure of cardiac contractility.

The different types of heart failure resemble different diseases, with each having different therapies and challenges. The key problem of HFrEF involves a reduced contractility of the LV, which is usually accompanied by a diastolic dysfunction of said ventricle. Conversely patients with HFpEF commonly have, besides a diastolic dysfunction of the LV, also an impaired systolic function, as recently demonstrated, using more sensitive imaging modalities.(12) (*see 1.3.3, Left ventricular systolic dysfunction*) The diastolic dysfunction is characterised by a reduced compliance of the LV as well as an impaired active relaxation during the isovolumetric phase of the relaxation cycle. This leads consecutively to increased end-diastolic filling pressures of the LV(LV*EDP*) to sustain a required CO.

Compliance describes how easily a structure expands relative to a pressure change. It is therefore a size for ductility and, in the case of the heart, highly dependent on the relaxation of ventricle.(13,14)*(see chapter 1.3.2))*

HFmrEF was thought to resemble features of both diseases, (3,15) though recent evidence suggests a closer relation to HFrEF in regards to various clinical characteristics such as, but not limited to, treatment response and co-morbidities. One finding for example in the SwedeHF cohort study, which includes (as the name suggests) all HF patients in Sweden, was a comparable prevalence of ischemic heart disease (60.7% vs. 60% vs. 52.4%) as well as a previous ischemic myocardial infarction (68.7% vs. 71% vs. 56%) in HFmrEF and HFrEF, but not HFpEF.(16) In a post-hoc analysis of the CHARM-program

(*Candesartan in Heart Failure: Assessment of Reduction in Mortality and Morbidity*) a treatment response in HFmrEF patients, which was similar to HFrEF patients could be shown, for the endpoint CV death and HF hospitalisation.(17)

These pathophysiologic processes explain the old terminology systolic HF and diastolic HF. These older terms should be avoided since they imply only one common aetiology, which does not represent current knowledge. (18)

Since the evaluation of the HF subgroup in the Framingham study (19) in 1993, distinct therapy improvements have been made for patients with a reduced or mid-range LVEF. Conversely, during the same period, little progress has been made attenuating the impact of HFpEF.(3,20) (*see chapter 1.3.5*)

1.2.1.2 According to clinical severity

During the diagnosis of HF, symptoms are not only classified by their functional characteristics but also by their severity. The most common scale to quantify these symptoms is the "New York Heart Association Functional Classification" (NYHA), which categorizes patients from I (NYHA I), if no symptoms prevail during everyday tasks, to IV (NYHA IV) if signs and symptoms are present even at rest.(15)

1.2.2 Epidemiology of HF

In developed countries heart failure is affecting over 2% of the adult population, in 2012 alone in the United States more than 5.8 million individuals. (21) The syndrome disproportionately concerns the elderly, nearly 12% of the population over the age of 80 years are affected.(22) Likewise, individuals of low socioeconomic status suffer disproportionately more frequently from HF (adjusted according to age and sex 2% vs. 1.2% in the least deprived). In this study Conrad et al.(23) explained this correlation by a higher prevalence of comorbidities in those individuals. Comorbidities in HF are common and their number per patient is increasing. At diagnosis of HF on average 3.4 comorbidities per patient were present in 2002, whereas this number climbed to 5.4 in 2014.(23)

The lifetime risk for developing heart failure in North America reaches nearly 20% according to the Framingham study (19), thus contributing hugely to all cause morbidity and mortality in the USA and Canada.(19,21) Similar numbers are estimated to be true for Europe, with the only lager population-based cohort study being the Rotterdam study.(24) There the authors calculated a lifetime risk to develop HF for people over 55 years of age of 33% in men and 29% in women. (*see Figure 2*) (24) Due to the fact that only 50% of all

patients with signs of decreased left ventricular (LV) function in the echocardiography have symptoms, these numbers are thought be even higher. (25,26)

With age being one of the most important risk factors for developing heart failure, and an aging population in western countries, prevalence and costs are thought to increase, putting the social services under huge pressure. (24,27) Heidenreich et al.(21) predicted an increase in the prevalence by 23% until the year 2030, from 2.42% in 2012 to 2.97% or nearly 8.5 million patients in the US. By then the estimated costs are expected to exceed $160 billion annually. (21)

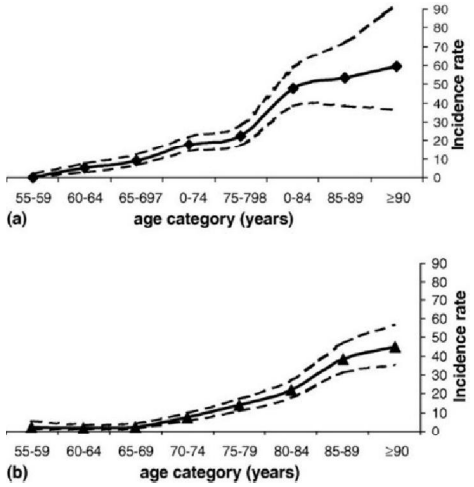

Figure 2 Age-specific HF incidence rates in men (a) and women (b) according to the Rotterdam study (24) (Incidence rate per 1000 person years, 95% confidence band), © *2004, Oxford University Press*

There is some conflicting evidence regarding the development of the incidence rate of HF, but the increase in prevalence is undisputed. Conrad et al. (23) reported a decrease in the age and sex adjusted incidence rate of HF between 2002 and 2014 by 7% (Incidence rate declined from 358 to 332 / 100.000 per year). But during the same period, the diseases' prevalence of the analysed cohort in the UK increased by 23%.

1.2.2.1 Epidemiology of HFpEF

Not only is the prevalence of HF in general increasing steadily, but also the distribution between the different subgroups is changing towards the phenotype with a preserved EF.

In a retrospective study including 6076 patients from a single centre in the US, Owan et al. (28) could show 2006 an increase in the HFpEF prevalence. In the first five-year period included in this analysis, (starting as of 1987), 38% of the patients did have a preserved EF. This relative proportion increased in the two following five-year periods to 47% and 54%, even after adjusting for age. During this 15-year period the absolute number of patients with

a reduced EF did not change significantly. (28) Based on this data it seems that the increase in HF is substantially driven by the increase in patients with a preserved EF.

A similar increase could be noted in AHAs "Get With the Guidelines-Heart Failure" initiative subgroup analysis by Steinberg et al.(29) During the analysed period the hospitalisation for HFpEF increased from 33% in 2005 to 39% in 2010, while at the same time those for a reduced EF decreased from 52% to 47%. (29)

Since the absolute numbers of patients with HF are thought to increase over the next decades (*see above, chapter 1.2.2, Epidemiology of HF*), as well as the relative distribution between the entities are expected to shift towards the HFpEF-phenotype, numerous authors are predicting a steep increase in its diagnosis, so that it will eventually become the most prevalent form. (18,28,29)

1.2.2.1.1 Mortality

Despite considerable interest by the industry as well as by public health initiatives for new therapy approaches, mortality is still unacceptably high. Depending on the study the 5-year mortality for HFpEF ranges between 65% (28) and 76% (30) and is thus significantly higher than of most malignancies. The average 5-year mortality in the US after receiving a diagnosis of cancer between 2008 and 2014 was 31%. (31)

Owan et al. (28) reported a decrease of mortality due to HFrEF during the studied period (*see Figure 3 (a)*), while it remained unchanged for the preserved EF-phenotype (*see Figure 3 (b)*).(28)

(a) **(b)**

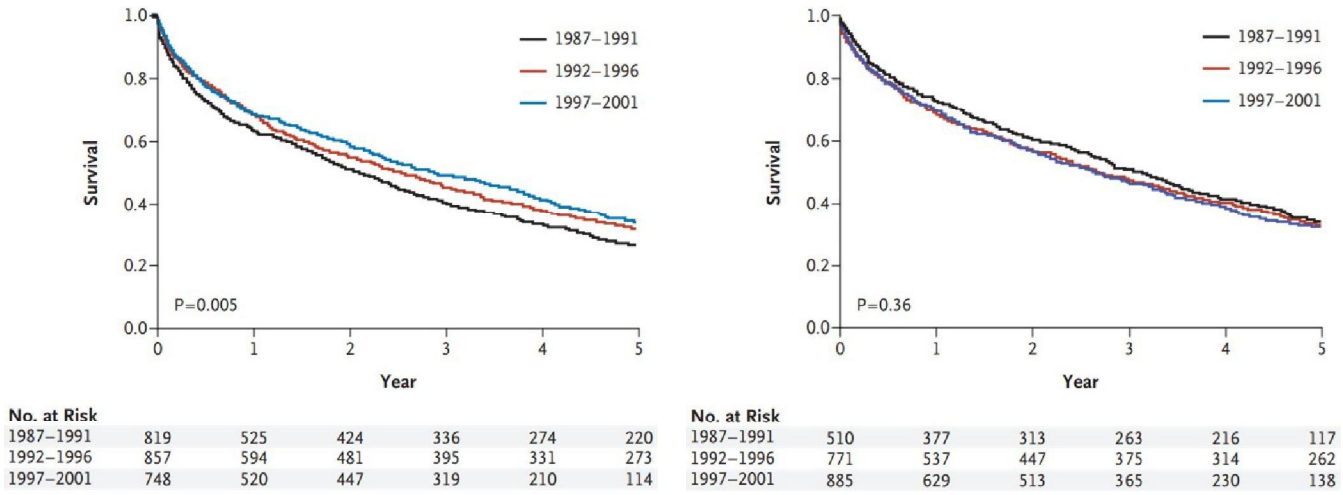

Figure 3 Kaplan-Meier survival curves for three 5-year periods of patients with (a) HFrEF and (b) HFpEF (28)

Reproduced with permission from (28), © Copyright Massachusetts Medical Society

1.2.2.1.2 Gender difference

In the EPICA trial (32), a cross-sectional observational study in Portugal in 1998, gender differences in the two different disease-entities of HF were systematically analysed. The authors could show a distinct difference between males and females regarding HF phenotype. In the overall population over 25 years of age, females were twice as likely to develop HFpEF (2.42% vs. 0.88%), as compared to male individuals.(32) (*see Figure 4*) These results are consistent with the findings reported by other authors. In Olmsted county Dunlay et al. (8) stated, that 63% of the HFpEF patients were of female gender.(8)

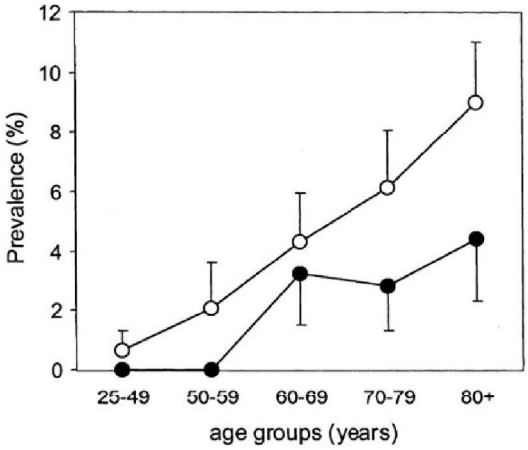

Figure 4 Estimated prevalence rates of HFpEF (● males, ○ females; 95% CI)

Modified from (32), © 2002 the Authors

Despite the higher incidence of HFpEF in female individuals, gender per se seems to be cardioprotective regarding cardiac endpoints. In recent years Duca et. al. (33) conducted a prospective observational study over a period of 6 years, beginning 2010. They analysed clinical and outcome data in individuals being treated by the Medical University of Vienna for HFpEF. Male individuals were more prone to die from cardiac death (16.5% vs. 6.1%), while all-cause mortality was not changed between the two groups, despite males suffering from more co-morbidities. Women tended to die more often from non-cardiac illnesses (10.5% vs. 2.5%), e.g. infections (23.3% vs. 0%). (33)

However, the association between gender and HFpEF remains controversial. A metanalysis of four different community-based cohorts could not identify an association between gender and development of disease. (34)

Considering current evidence, it can be concluded that the HFpEF is a heterogeneous syndrome, with female predominance, disproportionately affecting the elderly and estimated to increase over the next years.

Despite the research conducted in recent years in this field, all epidemiological data needs to be interpreted with caution. Nearly all bigger studies capture patients with HF using diagnosis related codes, which may give room to various confounders.(35)

1.2.3 Aetiology of HF

Since the definition of HF itself is very general, numerous conditions can result in the syndrome. Any illness causing functional or structural alterations to the heart, may ultimately end in HF.(5)

Most HF cases in high-income countries may be attributed to one of four underlying diseases: ischemic heart disease (IHD), chronic obstructive pulmonary disease (COPD), hypertensive heart disease (HHD) or rheumatic heart disease. Other diseases which frequently cause HF worldwide include valvular heart disease (both rheumatic as well as degenerative) and primary or secondary cardiomyopathies.(36) In a significant number of patients, up to 20-30% of those with HFrEF, the exact cause for the development of HF is unknown. (5)

1.2.3.1 HFpEF

The two subtypes, HFpEF and HFrEF differ regarding their aetiology, though there is a considerable overlap between the two groups.(5) Newer concepts like the obesity related HFpEF phenotype (37) are trying to define specific subgroups, in the hope of improving the understanding of the disease subsequently developing specific therapies.

1.3 Heart failure with preserved ejection fraction

As described above, the current classification of HF is relying heavily on the EF of the left ventricle as divider. To diagnose HFpEF, the ESC expects signs and symptoms in the presence of an EF equal to or above 50%. (*see Table 2*) Additional signs may include concentric hypertrophy of the LV, LA enlargement, LV diastolic dysfunction as well as elevated serum levels of N-terminal prohormone of brain natriuretic peptide (*NT-proBNP*) or brain natriuretic peptide (*BNP*). Dyspnoea, especially during exertion, is one of the most prevalent clinical symptoms in these patients. (3)

1.3.1 Risk factors

Various risk factors are known to increase the likelihood for developing heart failure with a preserved ejection fraction. What most of them have in common is association with a low grade systemic pro-inflammatory status, which is thought to be causal in the development of the disease involved. (*see 1.3.2 Pathophysiology*)

1.3.1.1 Age

As already described above, age is one of the key risk factors for developing HFpEF in developed countries, therefore prevalence of HFpEF is highly age dependent. Zile and Brutsaert (4) estimated, that in patients with HF and aged 50 years or younger, a preserved EF was only present in 15%, whereas in patients over the age of 70 years this number increases to 50%. (4)

1.3.1.2 Female gender

Female patients seem to be disproportionately often affected by HFpEF, when compared to their male counterparts. (*for more details see chapter 1.2.2.1.2, Gender difference)* However, the exact reason for this effect is unknown and recent evidence questions its existence. (34)

1.3.1.3 Comorbidities

In individuals suffering from HF, the vast majority is suffering from multiple comorbidities. In a study conducted by Chamberlain et al. (38) in Olmsted County/US, 86% of the patients fulfilled the definition of multimorbidity (≥2 diseases). This multimorbidity was even more distinct in the subgroup of patients with a preserved EF, compared with patients suffering from HFrEF. On average these patients suffered from one additional chronic disease. (4.5 vs. 3.7) Interestingly the pattern of comorbidities between the two diseases, as well as the distribution between the genders in HFpEF was comparable in the study. More than 50% of patients were suffering from hypertension, diabetes and arrhythmias. (38)

What most of the comorbidities have in common, is the fact that they cause a low grade systemic pro-inflammatory state, which is thought to be key in the development of HFpEF. *(for more details see chapter 1.3.2.2, Systemic inflammation and 1.3.2.3, Endothelial dysfunction)*

However, other authors could show a distinct difference in comorbidities. Owan et al. (28) identified the following risk factors being more prevalent in HF with a preserved EF:

- BMI coherently obesity (41.4% vs. 35.5%)
- Lower Haemoglobin (11.8 g/dl vs. 12.5 g/dl)
- Hypertension (62.7% vs. 48.0%)
- Atrial fibrillation (41.3% vs. 28.5%).

The following prevalence rates were less abundant in HFpEF:

- Coronary artery disease (52.9% vs. 63.7%)
- Substantial valve disease (2.6% vs. 6.5%)

Despite the seemingly reduced prevalence in relation to the patients with a reduced EF, these numbers are still significantly higher than in the general public. (39)

The importance of these risk factors is supported by an echocardiographic study conducted by Fischer et al. (40) The authors reported that, in the absence of any "predisposing conditions", HFpEF occurred in less than 1.1% and in individuals over the age of 50 in less than 1.2%. The highest attributable risk was atrial fibrillation (AF). (40) However, due to the close linkage between HFpEF and AF, some authors raise the question, if this dysrhythmia is a risk factor or a symptom of a common, underlying disease.(41)

A cause-specific hazard analysis of the PREVEND trial (42) underlines the aetiologic differences between HF with preserved respectively reduced EF. In the study the authors could only show increased risk between previous MI, increased hs-TnT, former smoking and the phenotype with HFrEF, but not HFpEF.

1.3.2 Pathophysiology

HF is a heterogeneous syndrome, therefore summarizing a common pathophysiologic pathway is difficult. In the subgroup of patients with a reduced EF, different drugs and therapies showed a distinct benefit regarding morbidity as well as mortality, implying at least a partially common underlying pathophysiology. This effect seems largely independent of aetiology or comorbidities.(35) HFpEF may be missing this common pathway, which would explain to some extent the fact that so far no therapy has proved beneficial for survival or relief of symptoms. (35) (*cf. 1.3.5 Established therapies*)

As the definition of the ESC aptly describes, the key characteristic of HF is the inadequate cardiac output (CO), which may exist at rest or during stress, leading to signs and or symptoms of the syndrome. This is usually accompanied (at least during exercise) by an inadequate increase in intracardiac pressures, which are needed to sustain an increased CO.

The predominant cardiac problem in a patient with HFpEF is the inadequate ventricular stiffness during diastole. A quantification of the systolic functions using the EF falsely suggests a normal systolic function. In recent years, with the utilisation of superior imaging modalities capable of describing the systolic function of a heart more adequately (such as speckle-based strain analysis), it is now widely accepted that the contraction is defective as well. (3,12)

When presented with an adequate diastolic volume at normal filling pressures, the ventricle is showing signs of an inadequate relaxation. This results in higher filling pressures to accommodate for a required SV and subsequently to an inadequate (under-) filling of the ventricle. This in turn leads, together with systolic perturbations, to a reduced antegrade blood flow (CO) and therefore causes organ dysfunction. These findings as well as symptoms (e.g., dyspnoea) aggravate especially during stress such as physical exercise, due to the higher demand for CO. (3,4)

1.3.2.1 Comorbidities

As already described in chapter 1.3.1, risk factors, comorbidities are highly prevalent among patients suffering from HFpEF. Most of these patients suffer from arterial hypertension (aHT). Therefore, chronic hypertension was thought to be the leading risk factor in the history of the disease.

Multiple effects are likely to contribute to the progression from arterial hypertension to HFpEF. One, previously thought as the most dominant one, is the direct result of the increase in the heart's afterload, leading to concentric hypertrophy and ultimately diastolic dysfunction (DD). A newer understanding of the disease's pathophysiology emphasizes the resulting inflammation as driving factor and puts aHT merely as one contributing factor.. (43,44)

1.3.2.2 Systemic inflammation

During recent years of research, the understanding of the importance of inflammation has deepened over time. As previously described (*see chapter 1.2.3*), there is a strong association between the comorbidities and the presence of HFpEF. Key associations were found to exist between HFpEF and arterial hypertension, obesity, hyperlipidaemia, age, diabetes and arthritis.(28,45) These are all pathologies which are known to go along with a low-grade systemic inflammation. They do not only increase the risk for HF, but emerging evidence suggests them as precursors of the disease itself. (43,46,47) Different pro-inflammatory markers are known to be elevated in patients with HFpEF, further underlining

the importance of an inflammatory component in the development of the disease. Elevated parameters include hsCRP, TNFα, Il-1, Il-6 of which the former can also be synthesized by non-inflammatory cells such as endothelial cells. This is interesting insofar, as a key role in progression of the disease is attributed to the endothelium. (46)

Even in the absence of a systemic inflammatory process (normal CRP-levels) an increase in inflammatory cells was described in endomyocardial biopsy samples of HFpEF patients. It was further shown that these immune cells secret TGF-β, which is known for its profibrotic effects. (*for further detail see 1.3.2.4.2, Extracellular matrix*) A result of the increased level of inflammation, was the markedly increase in reactive oxygen species (ROS), primarily in cardiomyocytes and endothelial cells. (48)

1.3.2.3 Endothelial dysfunction

Endothelial dysfunction (ED) refers to an activation of endothelial cells due to pathologic stimuli (e.g. inflammation, aHT, …) leading to altered relaxation, permeability, coagulation and cardiac performance. (49) ED is s a systemic process, therefore it also affects the heart.

The cardiac endothelium is comprised of the supplying vessels, both the large ones and the capillaries as well as the endocardium, which lines the chambers as well as atria.(46) Endothelial cells, especially those forming the capillaries, are thought to play a unique role in the pathophysiology of HFpEF. This is because they have direct contact to both, the blood as well as cardiomyocytes, propagating endocrine as well as paracrine signals to the tissue. (49)

Paulus and Tschöpe (43) summarized the cumulating evidence delineating a *"novel paradigm for heart failure with preserved ejection fraction",* attributing the development of disease to endothelial dysfunction. The frequently seen comorbidities such as COPD, arterial hypertension, go hand in hand with a systemic low-grade inflammatory process, over the course of time also affecting the endothelium. (*for more detail see above, chapter 1.3.2.2*) On the one hand, this endothelial inflammation would lead to endothelial expression of adhesion molecules and, subsequently, the migration of inflammatory cells, creating a self-propagating circle. On the other hand, due to the higher levels of circulating inflammatory cytokines, more reactive oxygen species (ROS) are produced. This oxidative stress in turn would impair availability of NO in the heart and ultimately lead to an extenuated level of cyclic guanosine monophosphate (cGMP) due to a reduced production. Lower levels of protein kinase G (PKG) ensue as a result, leading to CM hypertrophy, remodelling and decelerated relaxation of the individual cells, as well as the heart as such. All these factors

ultimately lead to increased LV filling pressures and signs and symptoms of heart failure. (43)

One finding in patients with HFpEF underlining the involvement of the endothelia, is the microvascular depletion of the heart. In a study conducted in the Mayo Clinic's tissue registry, hearts from autopsies of HFpEF patients were compared to those of healthy controls. Besides a higher number of comorbidities as wells as BMI, patients with HF had a reduction of microvascular density. The rarefication was evenly distributed across all myocardial layers and independent of the presence of epicardial CAD. MVD correlates with echocardiographic signs of diastolic dysfunction, which underlines the clinical importance of this finding. Furthermore the authors bring this finding in context with impaired oxygen-delivery, especially during stress, thus contributing to the development of HF. (39)

1.3.2.4 LV diastolic dysfunction

All the above-mentioned factors in turn may lead to HFpEF, which is mainly determined by the diastolic function of the ventricle. The one finding common in many patients with HFpEF at rest and in most during exercise, are signs of LV diastolic dysfunction. (46,50) One reason for this stress intolerance are the diastolic filling times, which decrease at higher heart rates, thus requiring a faster filling and relaxation. Thus normal LV filling pressures cannot be sustained at higher frequencies.(51) This often uncovers, at least at higher heart rates, a reduced diastolic reserve and ultimately leads to an increase in the EDP. (18)

Since the reduced relaxation capacity in the case of HF with preserved ejection fraction is attributed to the myocardial stiffening rather than pericardial or endocardial disease involvement, only two components of the heart influence the pathology strongly, the extracellular matrix (ECM) as well as the cardiomyocyte stiffness itself. (46)

The importance of diastolic dysfunction is undisputed, but it is still unclear why only a subgroup of patients with diastolic dysfunction become symptomatic and progress to heart failure. (40,52)

1.3.2.4.1 Cardiomyocyte stiffness

Only in recent years the strong impact of cardiomyocytes on myocardial relaxation was discovered. Up until then it was thought, the main defining feature of the mechanical properties of the ventricle were the ECM and, above all, the deposition of excess collagen. Chung et al. (53) could prove that in a mouse with the genetically altered protein Titin (resulting in a reduced elasticity of said protein), myocardial stiffening was happening in the

absence of an altered ECM. The authors removed parts (9 of the 15 Ig-like domains) of the immunoglobulin (Ig) segments which, under physiologic conditions, are the dominating factor of Titin's and thus cardiomyocyte's elasticity. While the collagen deposition was equal between the WT and KO mice, the in vitro and in vivo diastolic stiffness was reported to be significantly increased. (53)

Titin. This protein is one of the biggest known mammalian proteins (~2.5 MDa) and is thought to be one of the key determinants of diastolic tension in cardiomyocytes. (54) Titin is anchored on the one side to the Z-disc, while the other side is connected on the M-band. Parts of the protein, more precisely the I-band region, act as powerful bidirectional spring, making it key for the recoil in unloaded (e.g., single-cell experiments) conditions. This recoil happens if the contraction of the cardiomyocytes brings the sarcomere length below the slack length and is therefore also happening to a certain extent in vivo as this recoil also helps with the diastolic "suctioning" as part of the myocardial filling process. The mechanical properties of the protein depend on the exact composition of the I-band, therefore also the isoform, as well as posttranslational modifications, as for example phosphorylation. (55,56) Posttranslational modifications are thought to be besides bridging inside of Titin as well as acute energy deficits one of the main parts of acute heart failure. (46,50)

Cardiac energetics. Studies conducted by Phan et al. (50) on patients suffering from HFpEF could detect a distinct reduction in the cardiac energy level, when compared to healthy individuals. The group used - amongst other diagnostic modalities - cardiac magnetic resonance spectroscopy (MRS) to detect a changed ratio of creatine phosphate (PCr) relative to adenosine triphosphate (ATP) concentration, which can be used as an indicator of the cardiac energy state. (50)

1.3.2.4.2 Extracellular matrix

The ECM composition of patients with HFpEF is often, but not always, significantly changed, resulting in a stiffer ventricle. Both in animal models, as well as in tissue samples of patients who suffer from HFpEF, a significant increase in collagen can be detected. (39,46,48) Westermann et al. (48) compared endomyocardial biopsies from healthy individuals with those of patients suffering from HF. In the study the amount of collagen as well as the shift of the type towards the stiffer type I correlated to the extent of diastolic dysfunction. Furthermore, the group could show an increase in serum markers for collagen degradation, as well as production, which suggests a higher turnover. Despite the mentioned increase in the collagen degradation products, the authors reported lower levels of matrix metalloproteinase - 1 (MMP-1) and an increase in the enzyme tissue inhibitor of

metalloproteinases - 1 (TIMP-1). In a primary cell culture of patients' fibroblasts, the authors could show an increased synthesis of collagen type 1A1 mRNA and a transdifferentiation towards myofibroblasts in response to a stimulus with TGF-β. Therefore they explained the changes to the ECM primarily with the effects of TGF-β.(48)

Krüger (46) hypothesized that acute changes in the diastolic tension (as in acute heart failure) may be more strongly impacted by changes to the cardiomyocytes itself, (*see 1.3.2.4.1, Cardiomyocyte stiffness*) while in chronic situations changes to the ECM may prevail.

However, the contribution of fibrosis to the development of HFpEF remains controversial. In a study by Mohammed et al. (39) the authors could show no difference in the degree of fibrosis between HFrEF and HFpEF patients, despite the significant difference in systolic respectively diastolic dysfunction. These findings further stress the influence of relaxation in the development of heart failure with preserved ejection fraction.

1.3.3 Left ventricular systolic dysfunction

As the name HFpEF implies, the LV systolic functions seem to be normal. However, more recent studies, using more advanced imaging modalities, could detect subtle signs of systolic dysfunction. In a study comparing healthy age matched subjects to HFpEF patients, Phan et al. (50) could show an extenuated exercise induced increase in LV end-systolic elastance besides other disease specific features.

More recently a study conducted by Kraigher-Krainer et al. (12) compared patients with signs of heart-failure with a preserved ejection fraction to healthy controls on the one hand and to hypertensive heart disease patients with diastolic dysfunction, but without signs of HF on the other hand. The authors assessed the systolic LV function not only by LVEF, but also by strain analysis using a speckle tracking methodology. Though the patients with heart failure presented with a similar EF, their systolic function, assessed by the more sensitive longitudinal (LS) and circumferential strain, was highly impaired when compared to healthy controls. This difference was more pronounced in the LS and also true when compared to matching patients with diastolic dysfunction in the absence of HF. Contrary to patients with signs of HF, those with an asymptomatic diastolic dysfunction had an increased circumferential shortening. In the studied cohort these signs of a systolic function impairment were present in nearly two thirds of the HF patients and independent of the diastolic function. Furthermore the authors were able to show that worse strain correlated inversely with the NT-proBNP levels. (12)

1.3.3.1 Exercise intolerance

The impact of the systolic dysfunction seems to be especially strong during exercise. In a study conducted by Abudiab et al. (58), comparing HFpEF patients to healthy controls, distinct differences could be noted. The test persons were subject to haemodynamic evaluation at baseline as well as during exercise. While at rest only elevated filling pressures could be noted in the patients suffering from HF, exercise aggravated the picture strongly. The HFpEF patients could not increase their heart rate, cardiac output (CO), stroke volume and EF adequately, leading to a decreased maximal oxygen consumption, as well as a strong increase in the LV filling and pulmonary artery pressures. (58) This suggests that the increase in LV pressures, especially during exercise, can be attributed not only to the reduced diastolic reserve (*see 1.3.2.4, LV diastolic dysfunction*), but also to the inability to increase CO. This leads in turn to inadequately emptied ventricles and consecutively backwards failing, also supported by the above mentioned exercise induced increase in pulmonary artery pressure. (46,58)

1.3.4 Diagnosis

As described above (*see chapter 1.2*) the diagnosis of HF requires per definition a clinical correlate, so it heavily relies on the past medical history of a patient, the physical examination and subsequently the ECG. If there is the suspicion of HF a lab-workup of the patient, including NT-pro-BNP if available, or if not, any other natriuretic peptide. These laboratory tests should only be used to rule out a patient – not vice versa, since they feature a good negative predictive value, but lack an adequate positive predictive value. (3,59)

If the laboratory-results confirm the suspected HF (current ESC-cut-offs: *BNP >35 pg/mL* and/or *NT-proBNP >125 pg/mL*), an echocardiography should be conducted. Per definition for a patient to be diagnosed with HFpEF, the LVEF must exceed 49%. (*see chapter 1.2.1.1.1, Ejection fraction (EF)*) The current guidelines also call for <u>structural</u> (*e.g., signs of hypertrophy - left atrial volume index (LAVI) or LV mass index (LVMI)*) or <u>functional</u> (*e.g., signs of an altered relaxation E/e', mean e'$_{septal}$, LS or of an increased pulmonary artery pressure such as tricuspid regurgitation velocity (TRV)*) alterations to be detected. The ESC guidelines call for *stress testing* to be used to demask borderline findings. (3) If the tests render inconclusive results, stress testing or invasive diagnostics (e.g. Left ventricular end diastolic pressure (LVEDP)) may be performed. (3)

In accordance with the ESC's (above summarized) recommendations Pieske et al. (60) proposed a stepwise approach utilizing a diagnostic score to facilitate a better diagnostic process of HFpEF.

1.3.4.1 HFA PEFF score

In the "*HFA–PEFF diagnostic algorithm*" Pieske et al.(60) propose a diagnostic score, thus not relying on a single pathological finding. Therefore, non-classifiable patients as well as parallel diagnostic pathways, yielding - in the worst-case - conflicting results, should be avoided.

The stepwise approach starts with the screening and assessment of eligible patients (*i*) ("**P**re-test assessment"), who present with signs and symptoms compatible with the diagnosis of HF(pEF). The aim is not to "miss" any patients. To do so, different tests are recommended, which hardly differ from the ESC's suggestions. (*Signs and symptoms, ECG abnormalities, laboratory tests including natriuretic peptides (NP), echocardiography, exercise tests where appropriate*) If the suspicion substantiates, (*ii*) a formal **E**chocardiography (assessing both functional and structural alterations) and NP should be conducted. Based on the findings and by means of the HFA-PEFF score, the patients are grouped, into one of three categories, (*a*) HFpEF diagnosis confirmed (≥5 points), (*b*) further evaluation required or (*c*) HFpEF highly unlikely (≤ 1). For patients from group (b), whose risk of suffering from HFpEF is intermediate, the authors recommend a **F**unctional assessment to detect haemodynamic perturbations. If invasive measurements yield definitive results, the diagnosis can be made. Otherwise stress testing by means of echocardiography should be used. The results should then be entered into the HFA-PEFF score, leading to a reclassification of the patient. If there is concern about the validity of the results, the authors recommend the use of invasive haemodynamics. Once the diagnosis is confirmed, underlying (**F**inal) aetiologies should be considered and, where appropriate, treated.(60)

1.3.5 Established therapies

1.3.5.1 HFrEF

The therapy of patients suffering from HFrEF strongly relies on neuro-hormonal inhibition and especially on the Renin Angiotensin Aldosterone system (RAAS) as well as a blockade of the β_1 receptor. It could be proven in numerous trials that this pharmacologic approach not only improves signs and symptoms of the disease, but also prevents hard endpoints, such as mortality or hospitalisation. Therefore, numerous authors hypothesize that most patients suffering from this heterogeneous syndrome have a common underlying pathway, involving the RAAS in the pathogenesis of the disease. The basic treatment strategy for all HFrEF patients as recommended by the ESC (3) includes the following modalities:

Underlying disease. If specific, treatable diseases (e.g., Ischemia due to CAD) are the underlying pathology, these should be treated accordingly with the appropriate medical intervention. (e.g., Revascularisation, lipid lowering therapy, …)

RAAS inhibition. *Angiotensin-converting enzyme inhibitors (ACEi)* are recommended in all symptomatic patients as well as asymptomatic ones with signs of a systolic dysfunction unless intolerances exist. These drugs inhibit the conversion of the Angiotensin I to its final form, Angiotensin II. This exhibits several beneficial effects, such as lowering the blood pressure (BP) and inhibiting the ventricular remodelling. *Mineralocorticoid receptor antagonists (MRA)* inhibit the effects of Aldosterone, and are recommended in patients who are still symptomatic, despite the use of ACEi and β-blockers.

β-blockers. The ESC recommends this substance group as complementary therapy to ACEi. These drugs inhibit the cardiac specific isoform of the β- receptor and therefore block the effect of most catecholamines. (*for effects elicited by catecholamines cf. chapter 2.2.3.2.1, Isoproterenol*)

Diuretics. The ESC's current guidelines on the treatment of HF recommend the use of these drugs only as add-on to ease symptoms in the context of digestion. (3)

1.3.5.2 HFpEF

In contrast to the well-established therapy of HFrEF patients (*see above, chapter 1.3.5.1, HFrEF*), the pharmaco-therapy involving a blockade of the neuro-hormonal axis yielded no outcome-benefit for patients presenting with a preserved EF. Other pharmacologic approaches based on pathophysiological findings in animal models and human tissue samples were investigated, though similarly none yielded a significant mortality benefit in humans. (3,20)

Therefore, in the absence of a beneficial causal pharmacotherapy, the current guidelines emphasize the control of risk-factors as well as symptoms. This is especially important as most HF-patients with a preserved EF suffer from a significant number of comorbidities. Compared to HFrEF these comorbidities are more often the reason for hospitalisations. Thus the guidelines emphasise the treatment of these underlying disease as one key factor. (3,61) In view of the higher age, as well as morbidity of the patients and the high burden the disease puts on patients, the ESC puts a considerable weight on symptom relief. Especially diuretics should be considered in case patients are presenting with symptoms of congestion. (3)

Numerous theories try to explain why it proves challenging to find a pharmacotherapy with a significant benefit to these patients. One possible is the heterogeneous pathophysiology of the disease. Therefore, some authors argue, the syndrome may not have a (partially) common pathway among all patients, which could be targeted with a drug therapy. (*see chapter 1.3.2*)(35)

Another possible explanation by the ESC (3) involves the time of the pharmacologic intervention. The diagnosis of HF requires the presence of symptoms. Therefore the authors suggest that patients may be treated (in the history of disease) too late to sustain a benefit with regard to mortality. (3)

1.3.6 New therapy concepts

Numerous clinical trials as well as preclinical research focuses on the so far unmet need for a novel cure for HFpEF, both by pharmacological as well as interventional means.

1.3.6.1 Interatrial shunt device (IASD)

One of the pathophysiological hallmark features of HFpEF in the development of the disease is the increase in LVEDP and consecutively of left atrial pressure (LAP). The pressures often remain normal at rest, but physical activity and the demand for an increased cardiac output (CO) unmask the reduced diastolic reserve of the LV, and therefore increasing pressures. (for detailed workup on the pathophysiology of HFpEF *see chapter 1.3.2*) The LAP pressure can be quantified by approximation, measuring the pulmonary capillary wedge pressure (PCWP). In patients with HFPEF the PCWP, if normal at rest, rises significantly during exercise, which correlates with changed outcomes. (62)

In absence of an effective drug therapy and based on computer modelling, Corvia Medical developed a device, mimicking an atrial septal defect (ASD). (*see Figure 5*) Based on simulations, the company calculated a shunt diameter of 8-9 mm to be able to lower the average PCWP sufficiently, from 10 to 7 mmHg at rest, respectively 28 to 17 mmHg during exercise. (63)

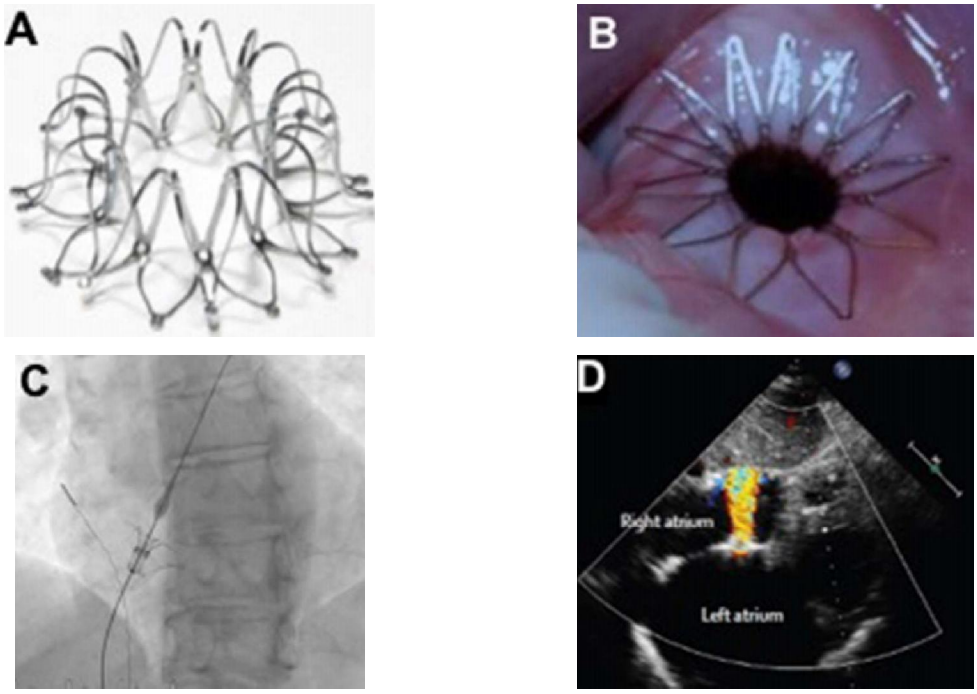

Figure 5 Pictures showing the IASD(64)
(A,B) Deployed IASD, **(C)** fluoroscopic image of the insertion, **(D)** TEE showing the artificial septal-defect blood flow from the left atrium to the right;
Modified from (64) under a CC BY license, © 2019 Kaye and Nanayakkara

So far only the results of the REDUCE LAP-HF study, a single-arm, nonrandomized open-label study, are available. Both, at six months and one year after the implantation of the IASD, a significant reduction in NYHA class as well as an improved quality of life and 6-minute walk distance test could be seen. (65,66)

Furthermore, in a follow-up analysis of the REDUCE LAP-HF trial (67), with a median duration of 739 days after the device implantation it could be shown that the observed mortality was lower than predicted. After three years the estimated mortality was calculated to be 10.2 deaths per 100 person years (95% confidence interval 6.1-16.9), whereas only 3.4 deaths per 100 person years (1.52–7.54) could be observed in the intervention group.

The suitability for all patients with HFpEF is reduced, because the procedure requires an invasive approach consisting of a trans-septal puncture of the RA *(see Figure 5 C)*, as well as a simultaneous transoesophageal echocardiography (TEE). In addition, there is a significant risk of thrombosis as a foreign body is placed in the heart to keep open the septal defect *(see Figure 5 A, B)*. Therefore lifelong low dose Aspirin therapy, as well as a short-term Clopidogrel therapy is required. (64)

The results of the unblinded study seem to be promising as well as safe, but due to the need for an invasive procedure, and the life-long anticoagulation the results need to be

validated. The multicentre study "REDUCE LAP HF-II", a randomized clinical trial is currently recruiting, with resultsnot to be expected within the next two years.

1.3.6.2 Histone modifications

One pharmacotherapy that has emerged in recent years as a promising candidate to treat HF, is a group of small molecule drugs called histone-deacetylases inhibitors (HDACi). So far, the results need to be interpreted with caution, only preclinical data is currently available for the treatment in the context of HF. These drugs can alter the function and or structure of proteins as well as the gene activity or expression of a cell, without changing the DNA itself, which is referred to as "*epigenetic modification*". Contrary to most of today's therapies, this mechanism of action does not rely on pathways or receptor interactions and holds promise for treating various disease.

Histones. Initially, after the discovery of DNA in the year 1953 it was initially thought that the genetic material was stored in the cell without the involvement of proteins, which soon turned out to be wrong. As we know today, the DNA of eukaryotes is stored in the form of chromatin, a condensed complex consisting of DNA and proteins, both located in the nucleolus. One of the key structural components of chromatin is a group of proteins called "*histones*". They are highly conserved in the course of the evolution of eucaryotes, underlining their importance. (68,69)

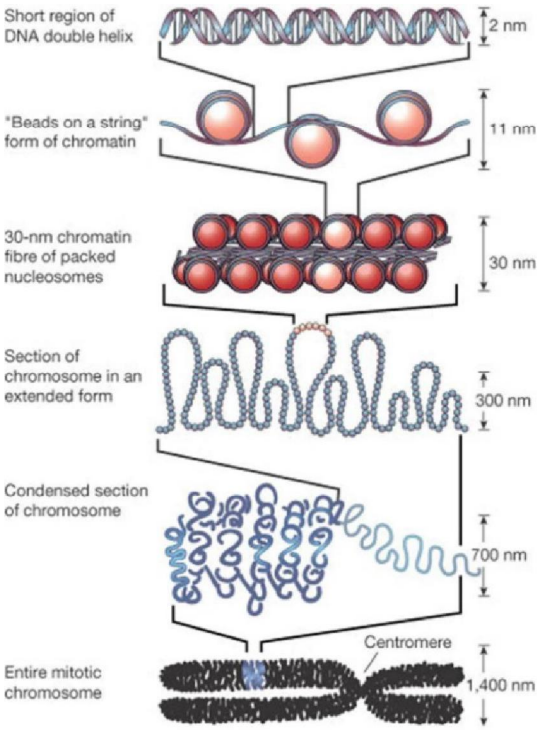

Figure 6 Organisational structure of a Chromosome (68)

Adapted/Translated by permission from Springer Nature: Springer Nature, Nature, Controlling the double helix, Gary Felsenfeld et al., © 2003, Nature Publishing Group

Chromatin Structure. Eight histones form an octamer, around which the DNA is folded in two turns, the resulting structure is now called "*nucleosome*". The exact composition of the different protein-subtypes depends on different factors, e.g., cell type or transcriptional activity. Numerous nucleosomes are arranged in series, connected through short strands of "*linker DNA*" forming *chromatin*. (*see Figure 6*) (68,69)

The DNA is compacted by a factor of approximately 50 until this step. As a result, the so condensed DNA is only poorly accessible to biochemical processes (e.g. enzymes as

the RNA polymerase or regulatory proteins), since signals or substances entering the nucleus encounter only the chromatin structure, not the DNA itself. (68,69)

Only as late as 1997 and with the help of high-resolution X-ray crystallography the exact structure of chromatin was finally deciphered. During the analysis, a protrusion of histone-tails was detected, so besides through the linker-DNA, two adjacent nucleosomes could make contact directly. Modifying these tails thus affects the three-dimensional shape and biochemical properties of chromatin. This process may happen spontaneously or may be catalysed by means of different enzymes, e.g. by histone acetyltransferase (HAT) and histone deacetylases (HDAC).(70) (*for more see chapter 1.3.6.2.2, Histone acetylation*)

1.3.6.2.1 Regulation of chromatin structure.

Since biochemical processes as transcription are essential to life, it is important to facilitate these reactions. Thus, chromatin cannot be inert, it must be a dynamic system with a regional change of the three-dimensional structure. All these changes are integral part of the epigenetic modifications of the genome.

Today there are three main known ways, how the expansion of chromatin and thus also alterations in downstream biochemical processes can be regulated:

Composition. The composition of the histone octamer itself can be due to the existence of different histone-subtypes altered, which facilitate diverse functions. Some of the protein-variants are known for their reduced stability, while others play a vital role in the repair of DNA breaks. (71,72)

Histone-tails. Furthermore, the histone-protein itself can be subject to chemical alterations by certain enzymes. Modifications both in the octamer-core as well as on the amino acid "tails" of histones protruding from the complex can occur, either adding or removing moieties. Thus, for epigenetic changes to be utilized different functions need to be executed. "Readers" decipher the information, "writers", put down the changes and "erasers" delete the changes. All of these are required for a cell to work normally. (73,74)

Chromatin remodelling complexes. Finally, chromatin remodelling complexes constantly change the exact location of a nucleosome, thus randomly presenting DNA-binding sites. Numerous complexes have been discovered until today, most of which work in conjunction with regulatory proteins, allowing them to bind selectively to certain regions. The process of remodelling requires the hydrolysis of ATP. (75)

The different mechanisms often work hand in hand. A chromatin-remodelling-complex may be required to uncover histone-acetylation binding sites.(68) The different

processes are not only important for their effect on transcription, but also repair, replication and recombination. (70)

1.3.6.2.2 Histone acetylation

As described above, the posttranslational modification of proteins is one of the key regulatory mechanisms in eukaryotic cells. This process was first described in the year 1963 as modifications to proteins of the histone family. Since then, multiple non-histone targets have been identified, making this biochemical process ubiquitous. More than 80% of all human proteins present modifications of the first amino acid. (76)

One of the most commonly modified amino acids is lysine at the ε-position, which may be methylated, coupled to ubiquitin or acetylated, of which the last presents the most common change. (77) The moiety is donated from acetyl-CoA or acetyl-phosphate (78), which leads to the neutralisation of the positive electrostatic charge, which in turn leads to a reduced electrostatic stability and changed DNA/histone interaction.(74)

The process of acetylation can occur spontaneously (e.g., to a certain extent in the mitochondria) or facilitated enzymatically. In biochemically relevant processes the latter prevails by far. (76)

Other amino-acids, which can be modified are arginine, which may be methylated and serine, which may be phosphorylated, but a myriad of amino-terminal changes are possible. (73,77)

Today 21 different lysine acetyltransferases (KAT) are known, which differ in the biochemical feature of the reaction, substrate, activity, and cellular localisation. (76)

1.3.6.2.3 Histone deacetylases (HDAC)

As described above, proteins may be subject to posttranslational modification to regulate biochemical processes. Some of these modifications may be reversed in a process involving another class of enzymes known as “Deacetylases”.

As the name suggests, these enzymes reverse the effect of HATs, resulting again in a positively charged lysine amino acid and thus local chromatin stabilisation. Supporting this theory is the fact that HDAC are associated with transcriptional repression. (70)

Today 18 different mammalian HDAC enzymes have been identified. They can be grouped into four distinct classes of HDACs and two different families. These families vary regarding their corresponding cofactors. To foster their reaction, the individual enzymes either use a zinc (Zn^{2+}) or NAD+ (only Class III) dependent mechanism. (79)

The different Zn^{2+}-dependent classes vary in different aspects, among others their binding-motif and activity. What they all have a common, is a highly conserved catalytic domain - apart from enzymes of Class IIa.(80)

The different classes are grouped according to their similarity to certain HDACs in yeast, while the denomination of the Zn^{2+}-dependent enzymes (classes I, II and IV) only correlates with the order of their discovery. (79)

Coupled proteins. By purifying cellular HDAC-complexes it could be shown that they do not usually exist on their own, but rather as part of large- multiprotein complexes. (73,81–83) For example HDAC 3 activity requires the formation of a complex with the *SMRT* (silencing mediator for retinoid acid and thyroid receptors; also known as N-Cor2) or *N-CoR* (nuclear receptor co-repressor) protein. In the experimental setting, the authors described that each compound on their own was not able to foster the reaction. The proteins' *DAD* (deacetylase activating domain) was needed to activate the catalytic activity. (82)

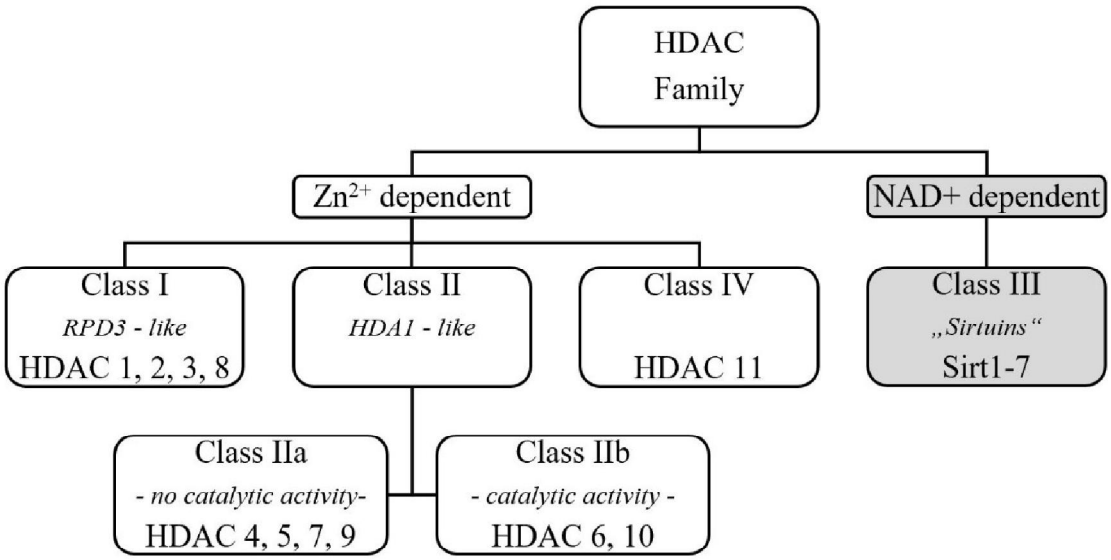

Figure 7 HDAC superfamily
White Zn^{2+} dependent, grey NAD+-dependent catalytic centre, *modified after (73,79,84)*

Class I

HDACs of this group have a similarity to the yeast enzyme "*Rpd3*". Their enzymatic activity is high, and they are localized in the nucleus, but can be found ubiquitously. As described above, they often form complexes with other proteins and most of their reactions happen in such a context. (84)

HDAC 1, HDAC 2, HDAC 3, HDAC 8

Class II

Enzymes of this class share similarities to the yeast enzyme "*Hda1*".(84) This class can be further sub-divided, based on their ability to facilitate the removal of acetyl-moieties directly. Enzymes of the subgroup IIa lack this activity, due to a mutation of the catalytic centre. The otherwise present amino acid Tyrosine was changed over the course of time to Histidine, rendering their enzymatic activity useless.(79,80) Nevertheless, they do fulfil a different, biologically important, function – the interaction with transcriptional factors – both inductors (e.g. MEF2-family, see below) as well as repressors.(79)

Class IIa. Apart from interacting with transcriptional factors enzymes of the Class IIa indirectly affect deacetylase activity of other enzymes by recruiting large multiprotein complexes. Fischle et al. (81) could demonstrate that the HDAC 4 fosters the combination of HDAC3 with the SMRT/N-CoR protein, thus activating the enzyme.

Enzymes of the class IIa were one of the reasons why the effect of HDACs in the context of the heart and heart failure were studied in more detail.(85) It could be shown, that HDAC 4 and 5 interact with MEF2 transcriptional family. Activation of the latter requires the dissociation with the help of the enzyme Ca2+/calmodulin-dependent protein kinase (CaMK). (86) MEF2 is known to be inducing muscle-growth (87) and thus seemed appropriate to target to counteract the pathological hypertrophy seen in HF. Accordingly the authors concluded that an inhibition of the HDAC would lead to severe hypertrophy. Antos et al. could show that the contrary was the case. Treatment of cells with pan-HDAC inhibitors (TSA, sodium butyrate) could reverse the features of stress stimuli, without decreasing the cell-viability.(88)

HDAC 4, HDAC 5, HDAC 7, HDAC 9

Class IIb. Enzymes of this class do have an enzymatic activity. HDAC 6 is highly abundant in the cytoplasm of mammalian cells and features, in contrast to all other HDACs, two enzymatically active sites. (84)

HDAC 6, HDAC 10

Class III

Enzymes of this class represent a special entity due to their differing required cofactor, NAD+. Class 3 enzymes are also referred to as "*Sirtuins*", due to the similarity to the yeast enzyme "*Sir2*". To this day, 7 different enzymes have been identified. (79) Due to the different cofactor, enzymes of this class are not affected by other pan-HDACi.

Sirt 1-7

Class IV

The only enzyme belonging to this class is *HDAC 11.*(84)

1.3.6.2.4 Approved HDAC Inhibitors on the market

The history of the discovery of the effects of HDACi is a lot older than the exact understanding of its mechanism of action. In the early 1970s Friend et al. (89) discovered, that, when incubating erythroleukemia cells with DMSO, more cells turned into differentiated normoblasts. She noticed a change in the protein-synthesis, as the cells turned red, suggesting the higher presence of haemoglobin and haem. This discovery led subsequently to the development of more potent substances, showing the desired effects, whilst not exerting cytotoxicity. The preliminary end products of this voyage resulted in the substances SAHA and TSA. (90)

Substances that inhibit the enzymatic activity of HDAC hold great promise as therapeutic option for various diseases. Up until this day there are six FDA approved substances, which inhibit deacetylase activity.(91) EUs EMA is more restrictive in the approval of HDACi. Only Panobinostat may be used in certain oncologic situations and Valproic acid is a treatment option in neurology. (92)

HDACi can be grouped in four different classes, according to their chemical structure. (*see Figure 8*) Most of today's approved HDACi are first generation HDACi, which means they do not show enzyme- and only little class-specificity. These enzymes exhibit a pan-HDAC inhibition by repressing the activity of multiple or all Zn^{2+} dependent isoforms. (73,93) (*for more see 1.3.6.2.3 Histone deacetylases (HDAC) and Figure 7*)

Due to the highly different expression profiles of the HDAC enzyme-isoforms and their wide range of different functions (*see 1.3.6.2.3 Histone deacetylases (HDAC)*), there is a reasonable interest of the industry to generate isoform- or class-selective drugs. There are numerous trials examining the effects of such medications, mostly in the context of varying malignancies and the results are awaited. (94)

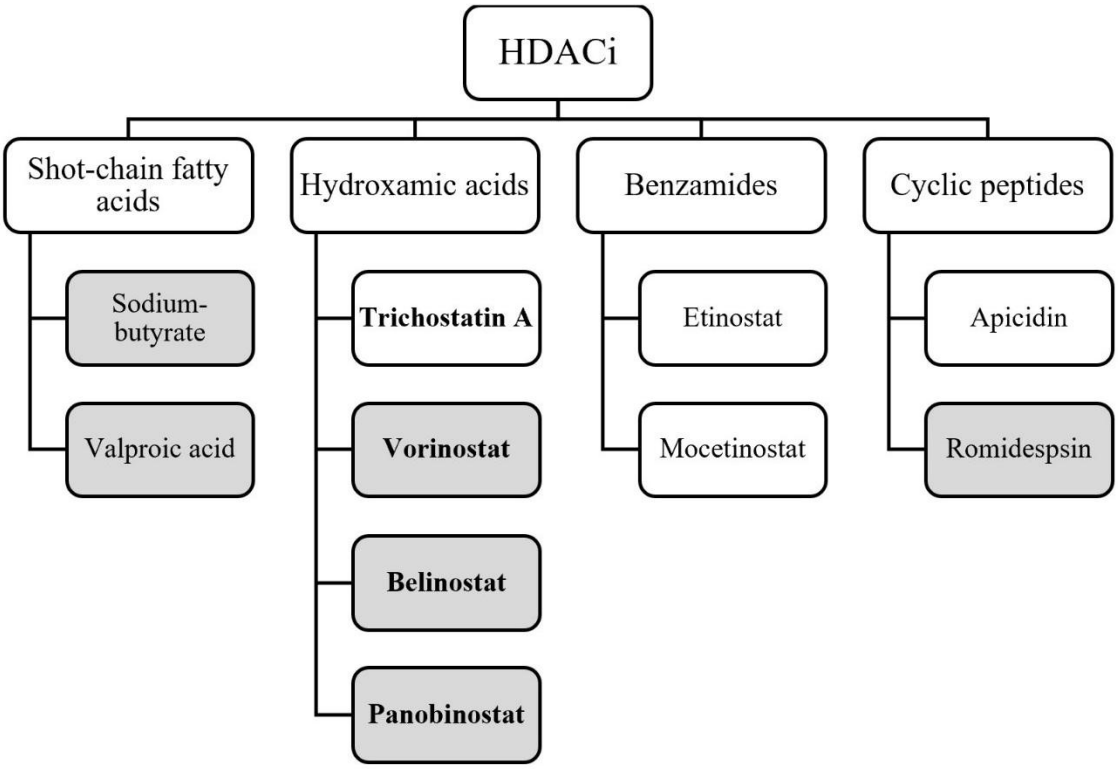

Figure 8 Exemplary HDACi grouped according to their chemical structure
(Bold panHDAC inhibitor, grey FDA approved substances), *modified after (91,93,94)*

Today's FDA-approved drugs may be used in treating following diseases: cutaneous T cell lymphoma, peripheral T cell lymphoma, multiple myeloma or neurological diseases. (91)

Typically HDAC-inhibitors, which inhibit Zn^{2+} dependent enzymes, consist of three parts: The "active" part of the molecule, which presents a zinc-chelating domain (which is in the case of Vorinostat and TSA the hydroxamic acid group) (90), a linker structure and lastly a recognition domain, which interacts with certain surface structures of HDAC. (91,93)

Besides trying to find HDACi with a better subgroup selectivity, the industry endeavours to find other, non-hydroxamic acid substances. Several hydroxamic substances are known to be mutagenic. (95) *(for more see below, 1.3.6.2.5, Vorinostat – Unwanted side effects)*

1.3.6.2.5 Vorinostat

Vorinostat or SAHA (abbreviation for "*suberoylanilide hydroxamic acid*"), is the first FDA approved HDACi. (94) The drug was licensed in the year 2006 and is sold in the US under the name "Zolinza". According to the company's package insert, it is indicated for the "*treatment of cutaneous manifestations in patients with cutaneous T-cell lymphoma who have progressive, persistent or recurrent disease on or following two systemic therapies*."(96) As the name of this class of therapeutics suggests, treatment results in

hyperacetylated proteins, both histones as well as non-histone proteins. This hyperacetylation is thought to be one of the causes of the desired effects in oncology, inhibiting tumour growth. It is known that certain cancers overexpress HDAC-enzymes and/or alter HAT, which is thought to contribute to cancer formation. (97)

Dosage. As most of the HDACi of the class of hydroxamic acids, Vorinostat shows a very potent competitive inhibition of the target enzymes. It has a fast onset of the inhibition within seconds. (90,98) The inhibitory constant K_i, as an indicator of a substance inhibitory potency (the concentration of a substance to reach a half-maximum inhibition(99)) was found out to be in nanomolar-concentrations. ($K_{i\ HDAC\ 1}$ 5.4 (±0.1) and $K_{i\ HDAC\ 3}$ 7.8 (±0.5) nM, 95% KI) (98) In oncology, usual concentrations which inhibit cell growth in vitro range from ED_{50} 0.5µM to 10µM. (97) However, the higher concentrations are reported to be challenging to reach, due to Vorinostat's poor solubility. (100)

Incubation time. Tiffon et al. (100) investigated the effects of Vorinostat in a cutaneous T-cell cancer cell line. They firstly determined the required concentration and duration by determining the acetylation of the Histone 4 at position K12 at various points in time (1h, 3h, 8h and 24h) and concentrations of Vorinostat (1µM, 3µM and 5µM). The authors reported a concentration maximum within 3h using a concentration of 5µM, after which a plateau was kept for 24h. (100) In cardiomyocytes derived from rats, an incubation time of 90' with a concentration of 2.5µM was previously shown to exhibit a strong acetylation, quantified by means of ac-tubulin measurement. (101)

1.3.6.2.5.1 Unwanted side effects.

Mutagenic potential. As described above (*see chapter, 1.3.6.2.4, Approved HDAC Inhibitors on the market*) some hydroxamic acids are known to be mutagenic. Therefore there is also considerable concern about Vorinostat's potential to damage the DNA, especially in the context of a chronic therapy. As with Vorinostat, Kerr et al. (102) could show a weak mutagenic potential testing the drugs in an Ames assay, but not with a 5-FU forward mutation test. Incubating a "Chinese hamster ovaries (CHO) cell line" with Vorinostat a significant increase of aberrations was present, but only at toxic concentrations. (incubation between 350µM and 700 µM for 3 hours) In normal human leucocytes no alterations could be detected. (102) The potential mutagenicity was more recently examined by Miles et al.. (103) The authors tested Vorinostat on a Hypoxanthin-Phosphoribosyl-Transferase (HPRT) mutation test assay. In this test the drug in question is added to an immortal cell line, together with the toxic synthetic purine base 6-Thioguanin. If cells survive, a mutation to HPRT's gene has most likely occurred, rendering the enzyme

inoperable and therefore the cells insensitive to the otherwise toxic metabolite. (104) Incubation with Vorinostat led to an increase in the mutation frequency, even at plasma concentrations of a tenth of the peak plasma concentrations seen in patients. These low mutagenic concentrations enabled 30-50% of the mutated surviving cells with a clonogenic potential. Similar results were reported by the authors for Romidepsin, another HDACi. This may suggest a hydroxamic independent, but rather HDAC specific mutagenic effect, which the authors argue may be due to a involvement of ROS. (103)

Unwanted side-effects in the above mentioned (*1.3.6.2.5, Vorinostat – Dosage)* dosing range in humans include anorexia, dehydration, diarrhoea, and fatigue. (105)

QTc. In the package insert of Zolinza (active ingredient Vorinostat) (96), the possibility of a prolongation of the QTc interval is described. In the phase I and II trials of Zolinza, including 116 patients, 5 patients were reported to have a prolongation of the QTc. (4 Grade II (470-500ms or increase of >60ms), 1 Grade III (<500ms)) (96) Another study conducted by Munster et al.(106)with the aim of assessing Vorinostat's effect on the QTc, reported no such effect. 24 late-stage cancer patients were subject to a single supratherapeutic dose (800mg instead of the standard dose of 400mg) of the HDACi. The serum concentrations peaked at 1.58µM, which equals roughly twice the usual concentration. The mean, placebo adjusted, change of the QTc did not exceed 10ms at any point in time during the monitored period of 24h. (106) Since the start of Zolinza there has been at least one case report of an adverse drug related event, in a patient experiencing an episode of a pulseless polymorphic ventricular tachycardia and a QTc of 826ms, during the treatment with the HDACi.(107) As part of the already mentioned preclinical safety assessment conducted by Kerr et al. (102), the authors examined the effects of Vorinostat on the potassium channel hERG in a CHO cell line. Changes to this ion channel, which may happen through interactions with various drugs, may lead to a prolongation of the QT(c) time and therefore increase the risk of arrhythmias. (108) The authors could detect only insignificant changes to the potassium current between vehicle and verum, even at concentrations up to 300 µM, which is roughly 300 times the therapeutic concentration. (102) The available evidence of Vorinostat's effect on the QTc time yields conflicting results. A QTc prolongation cannot be ruled out with certainty, but any given effect seems not to be strong.

Others. Though at higher drug-concentrations Kerr et al. (102) reported weight loss, as well as a reduction of food intake, diarrhoea and changes to haematologic parameters in treated animals. A significant, dose dependent, reduction of both the white blood cell counts

(WBC), especially lymphocytes, as well as the red blood count and haemoglobin were reported. Furthermore, the authors reported a lower platelet count and, in the serum biochemistry, a reduced total protein as well as globulin, all of which were reversible. (102)

1.3.7 HDACi treatment and HF

Treatment with SAHA in the context of malignancies has already entered clinical practice as therapy first and foremost for haematologic conditions, whereas in the context of heart failure results only exist in animal models. As already described above, treatment with HDACi holds great promise as new therapeutic strategy, both for HFrEF and HFpEF. This class of agents aims for a pharmacological pathway, different to established therapy concepts. These existing therapies for HF, which work by inhibiting the RAAS system, are known to be only beneficial in the context of a reduced EF, whereas HDACi work by epigenetic modifications. (*see 1.3.5 Established therapies*)

Since the discovery of the unanticipated cardiac effects of HDACi, numerous preclinical animal trials have shown a distinct benefit to diseases progression in modes of heart failure with reduced ejection fraction. Cumulating evidence, especially in large animals, holds promise for human trials.(109) In a large animal trial using a rabbit model of ischemia-reperfusion injury (IRI) Xie et al. (110) could show distinct beneficial effects of SAHA. The animals, treated with the HDACi had both a better fractional shortening, as well as a nearly 50% reduction of the infarct size. The cardioprotective effects of SAHA were primarily attributed to the increase in the autophagic flux, mainly in the border zone of the infarction.

Not only in HFrEF, but also in animal models of HF with a preserved ejection fraction, significant improvement of progression of the disease could be shown. In 2018 Jeong et al. (111) could show a new mechanism, improving relaxation in rodent models of diastolic dysfunction in the absence of modulating *(i)* blood pressure, *(ii)* cardiac fibrosis, *(iii)* hypertrophy or *(iv)* the giant protein Titin. Givinostat, a pan-HDACi, was able to prevent the development of diastolic dysfunction and bring LV end diastolic pressures back to normal in a DSS rat model. Cultured adult ventricular myocytes exhibited an accelerated relaxation when incubated with the HDACi. In myofibrils from DSS rats, treatment improved only the linear phase relaxation, a parameter of the inactivation of the thin filaments due to unbinding of Ca^{2+} and partial cross-bridge detachment. (112,113) This effect suggested a change to the acetylation status of said filaments being responsible for the accelerated relaxation. HDAC2 was found to co-localize with the myofibrils, reducing relaxation in vitro, while p300, a HAT, improved relaxation. The authors concluded

therefore that the observed improvement due to HDACi treatment was a result of the myofibrillar acetylation status, and not epigenetic modifications. (111)

A more recent work by Wallner et al. (113) explored the translational potential of HDACi treatment in a novel feline model of slow-progressive pressure overload (114), mimicking critical features of HFpEF. These animals developed a robust HFpEF like phenotype one month after surgery. These included LV hypertrophy, LA dilatation, diastolic dysfunction, elevated LVEDP, signs of LV systolic dysfunction in the radial strain analysis while having a preserved EF, elevated mean pulmonary artery pressure (mPAP) and signs of pulmonary dysfunction. (113,114) The authors started treating the cats 2 months post-surgery with the panHDACi Vorinostat, which halted the progression and partially reversed LV hypertrophy, LA dysfunction, elevated LV filling pressures, impaired radial strain and pulmonary function compared to vehicle treated animals. All these beneficial effects occurred in the presence of a pressure overload of the LV. The echocardiographic findings were further confirmed by invasive haemodynamics, which additionally revealed a normalized mPAP and LVEDP. To explain these finding the authors explored the relaxation of myofibrils and the findings match those previously described by Jeong et al. (111), namely an increased linear phase relaxation in large animals. (*see above*) (113)

Summarizing the current evidence, it is reasonable to conclude that Vorinostat shows profound improvements to hallmark features of HFpEF in animal models of the disease. Despite these undisputable findings, the exact mechanism of action remains poorly understood and can only be partially explained by the described nongenomic mechanism on myofibrillar proteins.

1.4 Aim and hypothesis

The aim of the experiments was to find out, whether the properties of Vorinostat to modify the contractile function can be reproduced in cardiomyocytes isolated from healthy C57/B6J mice and whether this effect can be linked to a change in the calcium transients.

Due to the central position of calcium, both for the contraction as well as for the relaxation of the cell, changes to the cell's calcium homeostasis could be one of the potential underlying mechanisms of action.

To explain the seen effects in the banded cats (Wallner et al.(113), *chapter 1.3.7*), we hypothesize that the cells in the treated group show a faster decay of the calcium transient, leading in turn to a faster relaxation of the cell. Furthermore, due to the faster reuptake, we expect the diastolic calcium levels to be decreased, which in turn should also be reflected in a larger diastolic sarcomere length.

1.5 Biologic importance of Calcium

As described above, calcium has a key position for both the contraction and the relaxation of a CM. It is essential to understand the role of Ca^{2+} in the muscle, as well as the key players involved, which all may be influenced by disease *(see chapter 4.3.2.2 Calcium kinetics)* or pharmacotherapy *(see chapter 2.2.3.2.1, Isoproterenol)*.

In the periodic table of elements calcium belongs to the metals and usually has an oxidation state of +2. Ca^{2+} the most abundant element of its group is in the human body and serves various essential functions. These range from its role as second messenger, to the formation of bone or teeth. The biggest proportion (99%) of the element in the human body exists as hydroxyapatite ($Ca_{10}[PO_4]_6[OH]_2$) mostly in bone, which provides structure and serves as storage. The calcium concentration in the plasma is usually tightly regulated at around 2.5 mmol/l, though the biologically important (unbound) concentration is lower. (1.25 mmol/l) (13) Due to the countless effects of calcium in a cell, the next paragraph only sums up the role of the ion to allow for a contraction of a single cardiomyocyte.

1.5.1 Excitation contraction coupling

The excitation-contraction-coupling of the heart describes the events that lead from the depolarisation of the cell to the contraction of the cardiac muscle and subsequently its relaxation. (115)

Key structures for the storage (and release) of calcium are the sarcoplasmic reticulum (*SR*) and the transverse tubules (*t-tubules*) of the sarcolemma. The t-tubules are invaginations of the sarcolemma into the muscle. Because of high concentrations of ion pumps (*Sodium calcium exchanger, (NCX)*) and channels (*Dihydropyridine receptors (DHPR) a type of L-type Ca^{2+} channel*) they play a crucial role in both the depolarisation and the repolarisation of a CM. The SR is a structure within the cell, allowing for the sequestration (*Sarcoplasmic/endoplasmic reticulum Ca2+-ATPase pump, (SERCA)*) and release (*Ryanodine receptor 2 (RyR2)*) of calcium. Both these structures are functionally closely related and located in very close proximity. Therefore, they are also referred to as "**cardiac dyade**". (13,115,116)

After an action potential results in a depolarisation of the cell, the DHPR channels open and allow for an inward calcium flux. The local increase of the cytosolic calcium concentration results in a conformational change of the RyR2 channel, leading to a sudden and more significant release of Ca^{2+} from the SR. In human CM most of the calcium (~70% of overall Ca^{2+}) is released from the SR, while only ~30% enter the cytoplasm via DHPR from outside the cell. This process of self-amplification is referred to as "**calcium induced**

calcium release". It is capable of increasing the calcium concentration of the cytosol inside of a human cardiomyocyte from 10^{-7}mol/l during the diastole by a factor of roughly 15 to a peak concentration of 10^{-5} mol/l during the systole. (13,115)

This increase of the cytosolic concentration of (unbound) calcium ion is the key step to allow for the **cross-bridge cycle** to happen. Calcium binds to the Ca^{2+} domain of the protein troponin C, subsequently causing a conformation change of troponin I, which moves tropomyosin. This exposes the high affinity binding sites for the myosin heads on actin. Thereby myosin undergoes a confirmational change, moving the actin filament towards the centre of the sarcomere. The myosin-head is released at the expense of one molecule of ATP, the myosin changes its shape and the cycle begins form the start. This continues unless there is no more ATP to release the myosin's head from the actin (as in rigor mortis) or unless the concentration of calcium decreases below a certain threshold. (13,117)

At concentrations below 10^{-7} mol/l the calcium ions dissociate from the protein troponin C, subsequently Tropomyosin again blocks the binding of the myosin heads at the actin filament and the crossbridge cycle is inhibited. (13)

Thus, for a muscle to relax quickly, it is key to clear the Ca^{2+}swiftly out of the cytoplasm. Due to a negative feedback loop, causing the DHPR channel to close upon a certain cytoplasmatic Ca^{2+} threshold this process starts already during the inward flux phase of calcium. (115) The **removal of calcium** relies on several active ion transporters and channels. The lion's share of Ca^{2+} is transported into the SR by means of the SR Ca^{2+}-ATPase pump (*SERCA*) and the secondary active $3Na^{+}/1Ca^{2+}$ exchanger (NCX), which removes calcium out of the cell. (13) These two pumps are responsible for >> 90% of the Ca^{2+}removal and are therefore tightly regulated. (e.g., *see chapter 2.2.3.2.1, Isoproterenol*) To a lesser extent the calcium removal relies on the plasma membrane Ca2+-ATPase (*PMCA*) and the mitochondrial Ca^{2+} uniporter. The latter transporter is an important regulator, as calcium entering the mitochondria is a stimulus for different enzymes, adjusting the ATP production to the current requirement. (13)

The ratio of each route on the clearing of calcium differs largely between different species. Therefore, results which were described for one genus do not necessarily need to be true in another one. (*see chapter 4.3.1.1, Ca2+pumps*)

2 Material and methods

To answer the scientific question of this thesis, a way of simultaneously recording contractility, calcium cycling of a cardiomyocyte, as well as its kinetics was required. Due to this fact the use of a multi-cellular experiment system was not feasible, so the use of a single-cell model was pursued. Cardiomyocytes are known to be notoriously difficult to incubate in a cell-culture and those immortal cell lines available on the market today all lack certain characteristics that would allow for conclusions based on mechanical studies.(118) Thus, it was necessary to use primary cells, for which the first and most important step is the isolation procedure.

One key advantage of using single-cell cardiomyocytes is the fact that this is a reductionist model, down to the single cell level. The recorded kinetics are independent of the influence of the ECM and therefore, only the direct effect of the treatment on one CM is visible.

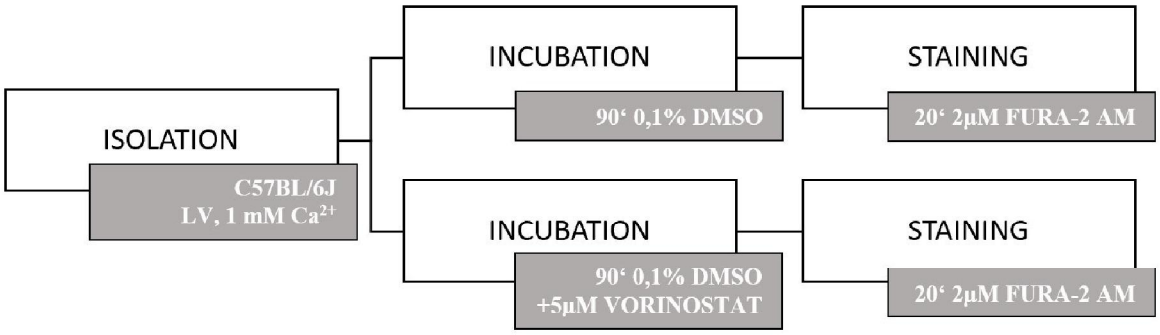

Figure 9 Preparation process of the single cell cardiomyocytes

2.1 Single-cell cardiomyocyte isolation

The term “single-cell cardiomyocytes” in the context of this thesis relates to the isolation for the consecutively following use (sarcomere kinetics and Ca^{2+} studies) of male murine ventricular cardiomyocytes.

Despite the fact that the use of single-cell cardiomyocytes for experimental studies is quite old, it remains challenging to isolate cells of adequate quality. So far, no single protocol has prevailed. (118,119)

One of the main advantages of using these cells is the possibility of simultaneously conducting imaging and mechanical studies, as well as studying cells of different differentiation, such as ventricular, atrial cells or cells of the electrical conduction system. (118) Furthermore, the use of gene-modified animals respectively their cells is reasonably easy possible, without any or with only minor changes to the protocol.

2.1.1 Isolation setup

The isolation setup varies widely from laboratory to laboratory. At first glance the goal seems simple. It aims to introduce a substance, which is capable of dissolving the extracellular matrix (ECM) surrounding the cardiomyocytes with as little damage to the cells as possible.

Isolation methods. On closer inspection a range of the challenges exists. One is to find a balance between cell yield and quality. Most enzymes cause a certain degree of damage to the cells, which is more pronounced with longer incubation times.

Regarding the introduction process of the digestion solutions two main ways need to be distinguished. One is a chunk approach, where the tissue is minced in pieces of 1-2mm^3 each and later put into a digestive bath. Alternatively, a retrograde aortic perfusion approach may be used. Here the coronaries of the heart are used to distribute the chemicals evenly throughout the tissue.

There are numerous pros and cons for the use of each of the two methods. For the laboratory conducting the experimentss the experience with retrograde perfusion for murine samples was decisive as experience proves to be of utmost significance regarding a good cell quality.

To reduce possible faults by the user, it was decided to simplify the existing setup so that it consisted only of the following parts:

- Syringe Pump
- 25ml Syringe (1)
- Light resistant perfusor line (2)
- Heat exchanger (4)
- Organ bath with Perfusion-catheter (5)
- Three-way stopcock (6)
- 2.5ml Syringe (7)
- Heating pump - inlet (3) | outlet (8)

Additionally required:

- 3 x 5ml glass beaker
- 2 x fine tipped tweezers
- Surgical thread size 5.0
- Microscope
- Pasteur pipette
- Falcon tube 50 ml

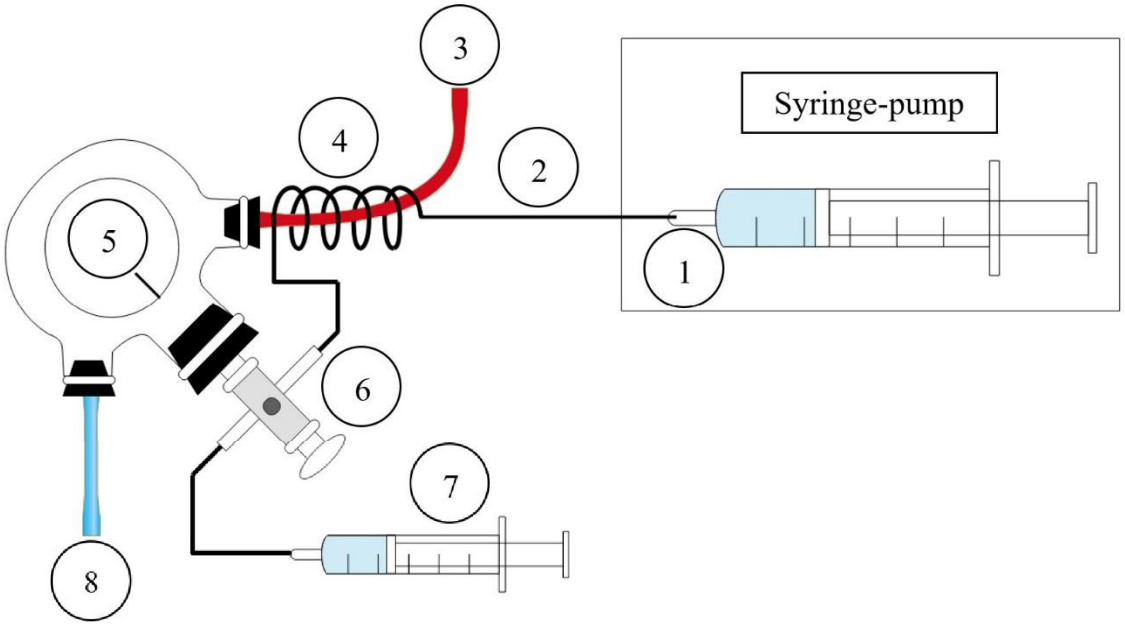

Figure 10 Schematic drawing of the modified retrograde perfusion setup for the of the mouse heart

Apart from being less prone to error the new setup has additional benefits: (1) less expensive glass ware required, (2) more precise times due to the predictability of flow and volume of the parts, (3) if required, sterile use easily achievable, (4) reduced quantity of the expensive enzyme solution required, (5) constant enzyme quality when heated just before the retrograde infusion, (6) constant temperature due to the heated organ bath.

2.1.2 Isolation protocol

It was noticed that the protocol respectively the exact times for the dissociation of the myocardial tissue to gain good quality cardiomyocytes is highly dependent on a multitude of different factors. As this process relies on enzymes, the impact of parameters which affect its kinetics such as the temperature, pH, and the age of the enzyme, as well as improperly flushed blood vessels were felt to be especially strong. Further effects which affect the outcome are contamination of the system, poor water quality and bubbles.(118) To have a consistent quality of the cells, special attention must be given to these factors.

2.1.2.1 Solutions

For the digestion of the heart two different solutions need to be prepared. Both are based on a buffer referred to as “perfusion buffer” (PB). For the detailed list of contents see Table 3.

Perfusion Buffer (PB)	
Compound	**Final Conc. [mM]**
NaCl	95
KCl	4.7
KH_2PO_4	0.6
Na_2HPO_4	0.6
HEPES-Na	20
Taurine	30
$MgSO_4$	1.2
Glucose	10
BDM	15

Table 3 Composition perfusion buffer

The perfusion buffer, as well as the normal Tyrode were prepared once a week, while the "Myocyte Digestion Solution" (MDS) and the "Myocyte Stopping Solution" (MSS) need to be prepared freshly for every isolation.

As the name suggests, the first solution is required to digest the ECM, while the second one is needed to stop the reaction and prevent an over-digestion of the tissue. The exact composition of the two can be found in *Table 4* (MDS) and *Table 5* (MSS).

Myocyte Digestion Solution		***[µl]***
	final volume[ml] **15.00**	**Final. Conc [mM]**
Liberase TM aliquot	72.00	-
$CaCl_2$ ***0.01M***	18.00	0.012
BSA *0.5M Stock*	450.00	15
Pyruvat *0.1M Stock*	750.00	5
Creatin ***[µg]***	11.25	5
Perfusion buffer ***[ml]***	13.71	-

Table 4 Composition of the Myocyte Digestion Solution (MDS)

Myocyte Stopping Solution		***[ml]***
	final volume[ml] **25.00**	**Final. Conc [mM]**
Perfusion buffer	22.47	-
BCS	1.25	-
$CaCl_2$ *0.01M Stock* ***[µl]***	*30.0*	12
Pyruvat *0.1M Stock*	1.25	5

Table 5 Composition of the Myocyte Stopping Solution (MSS)

BCS… *bovine calf serum (OrderNo. 12133C, Sigma-Aldrich, Merck, Darmstadt/DEU)*, BSA… *bovine serum albumin (OrderNo. A9418, Sigma-Aldrich, Merck, Darmstadt/DEU)*

The normal Tyrode is used to incubate and later perfuse the cells. It resembles a more physiological composition of electrolytes, including normal levels of calcium and lacks 2,3-BDM, a drug that hinders contraction. The reason for the "odd" composition of the perfusion buffer can be explained with the different requirements of the solution. With the PB

everything is done to keep the heart from contracting. This would damage the cells, as they lack oxygen as well as energy-rich phosphates in the absence of an adequate perfusion.

The contrary is the case with NT. Here the intention is to generate the best resemblance of the in vivo conditions of animals, to avoid any effects of the media on the cells and thus generating invalid data.

Normal Tyrode (NT)	
Compound	**Final Conc. [mM]**
NaCl	115
KCl	5
HEPES-Na	20
MgCl2	1
Glucose	10
$CaCl_2$	1

Table 6 Composition of normal Tyrode (NT)

The following solutions were prepared and frozen at -20°C to be thawed each time freshly. For FURA-2 AM it is very important to keep it protected from light at all times, since otherwise bleaching may occur, rendering the dye useless. *(for more info regarding staining and the mechanism of action see chapter 2.2.2, Indicator dye FURA-2 AM*)

Fura-2AM aliquot 	***[µl/µg]***
Compound	
Fura-2AM desiccated *[1001.86 g/mol]*	50 µg
DMSO	50 µl

Table 7 Preparation of FURA-2AM

Due to the high dilution required, the preparation of the Isoprenaline as well as Vorinostat aliquots cannot happen directly.

Similarly to Fura, Isoprenaline is an unstable compound when exposed to ambient light and temperature conditions so special precautions need to be taken. Otherwise, it disintegrates quickly.

Isoproterenol aliquot 	***[µl/µg]***
Compound	
Isoproterenol desiccated *[247.72 g/mol]*	24.8 mg
dd**H_2O**	10 000 µl
Final concentration Isoproterenol	10 mM
Isoproterenol 10 mM	10 µl
dd**H_2O**	9990 µl
Final concentration Isoproterenol	10µM

Table 8 Preparation of Isoproterenol

The last substance, which needed to be prepared for the experiments was the drug in question – Vorinostat. As it exhibits certain toxic properties, special consideration was given to avoid any contamination of staff or environment. Vorinostat has a low solubility in water, hence it was prepared in DMSO, which then was used to further dissipate it in NT. *(cf. 1.3.6.2.5, Vorinostat)*

Vorinostat aliquot	***[µl/µg]***
Compound	
Vorinostat desiccated *[264.32 g/mol]*	19.8 mg
DMSO	1500 µl
Final concentration Vorinostat	50 mM
Vorinostat 50 mM	200 µl
DMSO	1800 µl
Final concentration Vorinostat	5 mM

Table 9 Preparation of Vorinostat

Liberase (Roche, Basel/CH) is a commercially available blend of different enzymes. The type used, Liberase TM, contains highly purified Collagenase I and II, as well as the name giving Thermolysin in a medium concentration. Due to this, circumstance the usually significant batch-to-batch difference in enzymatic activity is decreased. Therefore, no adjustment of the digestion time is needed, when using new aliquots. (120)

Liberase TM aliquot 	***[ml/mg]***
Compound	
Liberase TM desiccated	50 mg
dd**H_2O**	10 ml

Table 10 Preparation of the Liberase TM

Due to the nature of the experimental setup as flow chamber on top of the microscope slide, the cells need to be continuously perfused with a liquid. In order to introduce new drugs, as well as keep the drug concentration steady in each group the prepared NT was divided into four flasks, each containing 100ml. The bottles were shielded from light and stored on ice. Corresponding quantities of the drugs (*see Table 11and Table 12*) were added and thoroughly mixed.

Perfusate Vehicle 	***[µl/µg]***
Compound	
Vehicle (DMSO)	100 µl
Normal Tyrode	100 000 µl
Final concentration	DMSO 14 mM
Vehicle (DMSO)	100 µl
Isoproterenol 10 µM	100 µl
Normal Tyrode	100 000 µl
Final concentration	Isoproterenol 10 nM
	DMSO 14 mM

Table 11 Ingredients of the ready to use perfusate vehicle

Perfusate Vorinostat 	***[µl/µg]***
Compound	
Vorinostat 5mM	100 µl
Normal Tyrode	100 000 µl
Final concentration Vorinostat	5 µM (+14 mM DMSO)
Vorinostat 5mM	100 µl
Isoproterenol 10 µM	100 µl
Normal Tyrode	100 000 µl
Final concentration	Isoproterenol 10 nM
	Vorinostat 5 µM (+14 mM DMSO)

Table 12 Ingredients of the ready to use perfusate Vorinostat

2.1.2.2 Preparation of the isolation setup

For the preparation of the setup firstly all in *chapter 2.1.2.1* described solutions need to be prepared. Secondly two 5ml glass beaker as well as the organ bath need to be filled with PB, after which the 2.5ml syringe is used to fill all perfusion lines with the same buffer. Special care needs to be taken to remove any remaining air bubbles in the system since they would inevitably lead to an air embolism of the connected heart. One 5ml beaker needs to be filled with MSS to stop the enzymatic reaction once the digestion is finished. Lastly, the 25ml syringe is filled with the MDS – since the enzymatic activity diminishes, the longer it is kept at ambient temperature.

Following the completion of the setup-preparation, the donor animal needs to be obtained. Twenty minutes before the organ collection the animal was heparinised to avoid clotting (100 I.E. UF-Heparin injection i.p.).

2.1.2.3 Organ collection

The following steps are time sensitive since the quality of the organ diminishes by the minute.

Induction of anaesthesia with Furan (Isofluran, Baxter) was performed, after which the animal was sacrificed by means of cervical dislocation. The thoracic cavity was opened, the heart exposed and freed from the surrounding tissue as well as the pericardial sack. Connecting blood vessels were cut and the organ collected.

Following the removal, the heart was washed by submerging it twice in the two previously prepared 5ml glass-beakers filled with PB, in order to reduce blood deposition in the following steps.

The following steps were performed using a stereomicroscope (Wild M5, Wild Heerbrugg AG) and fine-tipped tweezers. The freshly collected and washed organ was placed in the organ bath, the aorta primed, and the perfusion catheter inserted. It was attached by knotting a 5.0 surgical thread around the tissue surrounding the tip of the catheter.

2.1.2.4 Organ perfusion and tissue dissociation

Following the attachment of the heart to the catheter the process of perfusion started. The perfusion was always kept to a flow rate of 1ml/min.

Firstly, the blood vessels were rinsed thoroughly with a total volume of 4 ml PB (2.5ml syringe filled with PB + 1.5 ml of the perfusor lines).

Secondly, the enzyme solution, MDS, was perfused until a total volume of 6.5 ml was administered, after which the heart was dissected at the atrioventricular plane. Only the ventricles were removed, and the tissue transferred into the 5ml beaker pre-filled with the MSS. The tissue was minced with a pair of sharp scissors to a final size of 1-2 mm^3 and then dissociated, using a Pasteur pipette by pumping it up and down slowly. The resulting solution containing cells, detritus and remaining tissue was then filtered through a filter with a mesh size of 100µm, into a 50 ml Flacon tube.

Next the cells were washed and left to settle by means of gravity over a period of 5-10 min (exact time depending on the quality of the isolation), removing the supernatant without disturbing the pellet and resuspending it with approximately 5ml of MSS. This process was repeated twice, and the final volume brought up to exactly 10 ml.

2.1.2.5 Quality control

After washing the cells a second time, a sample of approximately 50µl cell suspension was collected for assessment under the microscope. To ensure an adequate cell quality, the experiment was only continued if the yield exceeded 50% of morphologically

intact cells. If the sample contained a high number of cells, whose cell wall looked "feazed up", or which did not resemble a "rod shape" or which had a highly granulated plasma, the isolation was deemed to be of minor quality and the isolation procedure was repeated. (*see Figure 11*)

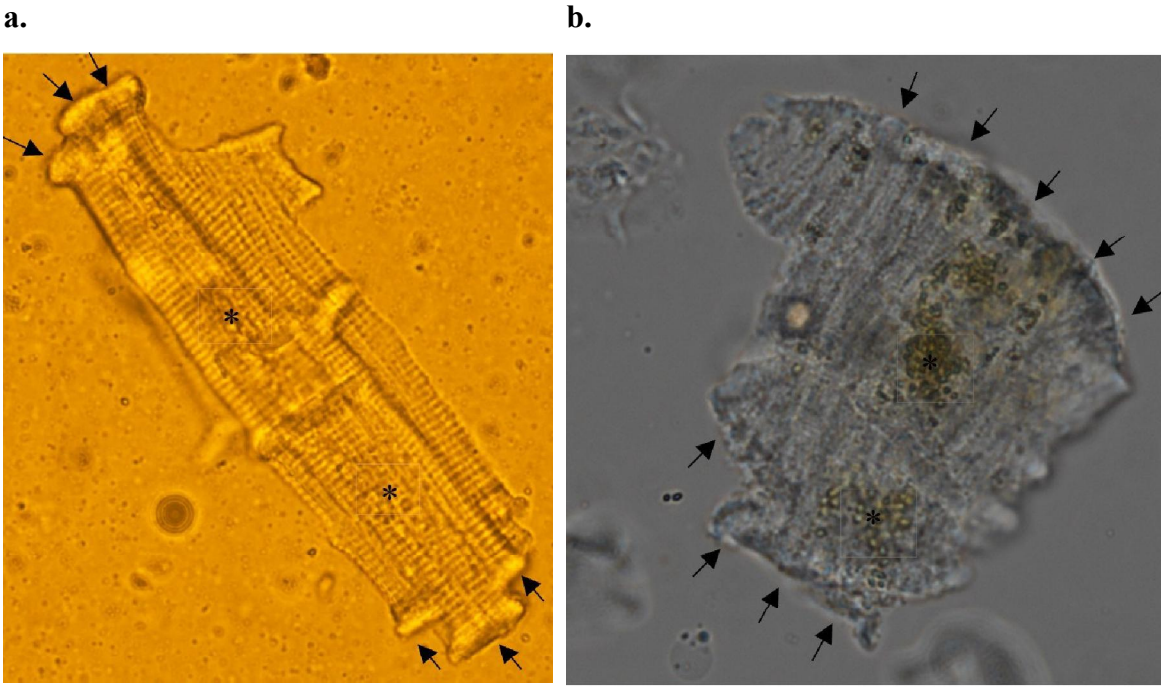

Figure 11 Pictures of morphologically unhealthy-looking cardiomyocytes
a. CM with two morphologic features, which suggest a dying cell – feazed up cell wall as well as a granulated cytoplasm; **b.** Different CM at a later stage. A highly granulated cytoplasm, a feazed up cell wall and a spontaneously a contracting cell can be appreciated;
The different colour results from different applied filters; (↖) feazed up cell wall, (*) granulated cytoplasm

2.1.2.6 Calcium rise

The next step is the rise in the media's calcium levels. This is a very sensitive step, since some of the cardiomyocytes, especially those with a damaged cell membrane, start to contract and eventually die. This effect has been a problem for a long very long time and still is. It is referred to in the literature as the "Calcium paradox". (121) It took nearly 10 years from the first publications of the isolation process in the early 70ies to the development of Ca^{2+}- tolerating CM. (119) Different causes and solutions have been proposed over the years in the literature with inconclusive results, but there is a strong emphasis on the importance of having a precise perfusion time with the low Ca^{2+} solution, as well as the slow rise in the ion afterwards. The calcium was gradually increased from the baseline level of 12 µM (in the MSS) to a final concentration of 1 mM free Ca^{2+} in four steps, each taking 4 minutes. After each of the increases the suspension was mixed carefully by inverting the Falcon tube.

Isolation in low Ca^{2+}

As already described in *chapter 2.1.2.1* "*Solutions*", the main reason for reducing the calcium level in the first place is to reduce damage to the cells due to spontaneous contractions, as there is no perfusion at this point in time ex vivo, allowing for an adequate homeostasis. Another important aspect is to facilitate the degradation of the ECM. Calcium plays an important role in the formation of the intercalated discs. It is necessary for the formation of the extracellular cadherin connection between two neighbouring cardiomyocytes. (122,123) The reduction of the calcium level to zero is not possible since the enzymes used in the digestion such as Liberase TM do require a minimal concentration to work properly. (118) A Ca^{2+} concentration of 12 µM is a good compromise between enzyme activity and cell protection.

2.1.3 Incubation with Vorinostat

1 ml of the freshly isolated cells was then incubated for 90 minutes in a suspension of MSS with a concentration of 5 µM Vorinostat suspended in 0.1% DMSO (1 ml Cell suspension + 1µl DMSO containing a concentration of 5mM Vorinostat) or vehicle (1 ml Cell suspension + 1µl DMSO). During that period, the cells were stored at room temperature.

2.2 Measurement of sarcomere Kinetics and calcium transients

As described above the need for simultaneously measuring calcium as well as sarcomere kinetics of the cell were a requirement for the measurement setup.

The commercially available myocyte calcium and contractility system by ionOptix allows for such functional characterisation of in vitro cardiomyocytes and was used in the experiments.

2.2.1 Measurement setup

The commercially available setup by ionOptix is compatible with the existing side ports of a wide-field (Nikon Eclipse Ti2, Vienna, Austria) epifluorescence microscope. (*see Figure 12*) This is equipped with a Nikon Super Fluor 40x/0.9 lens, allowing for magnification of the cardiomyocytes without the need to use an immersion oil.

The data acquisition process works as follows: A Xenon - light source generates a continuous stream of light, which enters the ionOptix "HyperSwitch". This device consists of a galvanometric driven mirror and two filters. The HyperSwitch has a switching rate of 250Hz and diverts the light beam through one of the two filters, with a passing frequency of 340nm and 380nm respectively.

The beam of light then enters the epifluorescence microscope through a side port (2) and is reflected by a semi-translucent mirror (4) onto the cell in question (3). There it excites the calcium-sensitive die Fura-2, which in turn emits light at a wavelength of 510nm. The excitation frequency depends on the calcium binding state of the Fura-2 die. (*see 2.2.2 "Indicator dye "*) Together with the optical image of the sample the light passes through the semi reflective mirror (4) and exits the microscope through another side port (4). There the emitted wavelength (510nm) is reflected by another semi-translucent mirror into a photo multiplier tube, which amplifies and later digitizes the signal. All other wavelengths, including the optical image of the cell, are recorded by a high-speed camera (7), which transfers the digital image to a computer for analysis.

1	Side port outlet
2	Side port inlet, 340/380nm in
3	Flow chamber
4	Semi reflective mirror #1
5	Photo multiplier tube "PMT"
6	Semi reflective mirror #2
7	MyoCam high-speed camera

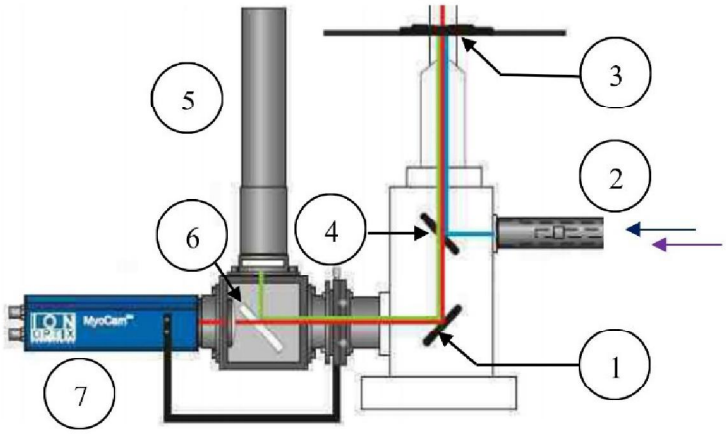

Figure 12 Schematic setup of the epifluorescence microscope with ionOptix acquisition module(124)
©IonOptix LLC

A miniature perfusion chamber is inserted in the space for the microscope slice, in which the cells can be characterised while being exposed to a constant flow of medium.

To introduce a drug, such as SAHA or Isoproterenol, the perfused media was changed. This change affected the flow-chamber approximately 40s later. After the measurements were conducted in one cell, the microscope-slice was cleaned and then refilled using the corresponding NT. The flowrate was always kept to 2.5 ml/min and the temperature to 34°C in the chamber. A higher perfusion rate affected the measurement quality and lead to an increased rate of cell-loss.

In the perfusion-chamber two Platinum – electrodes are located, which are used to pace the cells with an electric current. The corresponding current generator is called "MyoPacer" (ionOptix, Westwood/USA). The impulses were delivered at a frequency of 1 Hz and a duration of 5ms with a current of 20V.

2.2.2 Indicator dye FURA-2 AM

To measure the intracellular calcium concentration of a specific cell the ionOptix setup is designed to be used in conjunction with the indicator dye FURA2-AM. The ending "AM" refers to "acetoxymethyl"-ester, a moiety which makes the dye cell permeable. Once within the cell, the ester is removed by esterases, leaving the dye unable to exit through the cell membrane. (125)

The dye is a dual excitation indicator dye, which means it must be excited with UV-light at two different wavelengths. Depending on the binding state of calcium to the dye, these are 340nm for a chelated ion, or 380 nm in the absence of it. This double-wavelength excitation offers important benefits, since it reduces artifacts generated due to bleaching, uneven staining and leakage out of the cell. (126,127)

After the excitation Fura emits light at a wavelength of 510nm, which can be measured. The emitted energy directly correlates with the amount of bound respectively unbound calcium. (126)

Since the dye is light – sensitive, all handling, as well as storage must happen in the absence of light. The desiccated Fura-2AM was prepared in accordance with product information using Dimethylsulfoxid (DMSO) (OrderNo. A994.1, Carl Roth, Karlsruhe/ DEU) and stored at -20°C in 2µl aliquots. (for more information see *Table* 7) (126)

2.2.2.1 Staining

When the incubation of the cells with Vorinostat, respectively vehicle was finished, they were resuspended and 1 ml was transferred into one of the prepared Fura-aliquots, resulting in a final Fura-2 AM concentration of 2 µg/ml. The cells were stained for 20 minutes. To reach a more even distribution of the dye, the Eppendorf tube was stored sideways for 18 min. and only put upright for the last two minutes. Afterwards, the cells were washed twice with the corresponding batch of NT and finally resuspended in a final volume of 1 ml. Now that the staining was complete, the cells were stored in the absence of light and could be used for measurement.

2.2.3 Measurement

All measurements were conducted with freshly isolated, incubated, and stained cells. (*see above*) The tubes, as well as all hoses and the perfusion cell were filled with the NT corresponding to the group to be measured. (*for more see chapter 2.1.2.2*) For the measurement sequence see *Figure 15*.

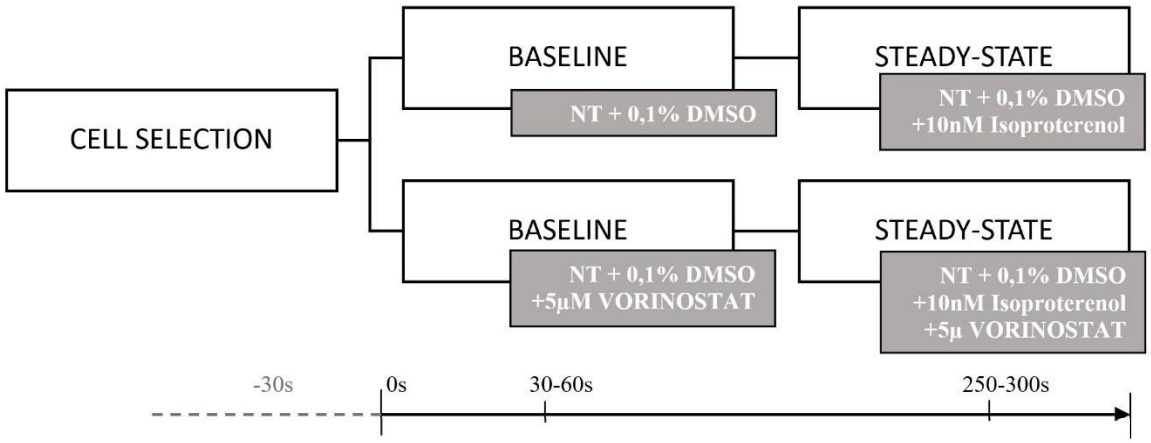

Figure 13 Measurement sequence with approximate corresponding times

2.2.3.1 Cell Introduction and Selection

The cells were resuspended and between 20 and 50µl of the suspension was transferred into the flow-cell. There they were left to settle at the bottom of the microscope slice for about 2-3 min. After that the perfusion was started and the MyoPacer was activated. An appropriate cell was selected, after which the measurement was started.

Criteria for the cell selection were the morphological appearance (*cf. 2.1.2.5* and *Figure 11*), no contact to other cells or debris, homogeneous contraction, no arrhythmia and no spontaneous activity without an electric stimulus during a period of 10s.

2.2.3.2 Measurement cycle

Each cell was then perfused firstly with the corresponding NT and then with 10nM Isoproterenol. Both times this was done until a steady state was reached. This was usually the case after 30-60s for the baseline measurement and 250-300s for the Isoproterenol stimulus. (*see Figure 15*)

The perfusate was stored protected from light and cooled with ice since the effect of Isoproterenol would otherwise diminish significantly over time.

Cells' kinetics as wells as calcium transients change significantly over the course of time after the isolation. To reduce the impact of this effect on the validity of the measurements, the groups were measured alternatingly after every two cells.

2.2.3.2.1 Isoproterenol

Isoprenaline, also called Isoproterenol, is an unselective β-sympathomimetic drug, (though for cardiac-related effects β_1-receptor activity of utter importance is) with hardly any α-adrenergic activity.(128) Therefore, Isoprenaline causes positive dromotropic, chronotropic, lusitropic and inotropic effects in the heart. For the experiments, conducted in

the context of this thesis, (measurement of single cell CM) only the latter two effects are relevant.

Isoprenaline induces the enzyme “Adenylyl-cyclase”, which increases the cytoplasmatic level of the second messenger cAMP, leading to an activation of cAMP-dependent kinases, notably the protein kinase A (PKA). This has in turn two main effects involving the transmembrane calcium flux: PKA phosphorylates proteins of the L-type Ca^{2+} channel, leading to an increased influx of calcium, which in turn enhances the myocard’s contractility. The faster relaxation is caused by a faster clearing rate of the calcium, due to the enhanced efficacy of the ion transporter SERCA. This is triggered by an increased phosphorylation of the protein phospholamban. However, there are numerous other effects which are caused by the beta-sympathomimetic effect of Isoproterenol. (13,128,129) (*see chapter 3.3, Diastolic hallmarks*)

For these reasons Isoproterenol is used in the context of experiments using single cell cardiomyocytes to increase the “gain” and therefore to unmask otherwise hidden changes to the cell.

2.2.4 Analysis

To avoid any bias, the analysis of the traces was only performed after all measurements had been conducted.

2.2.4.1 Data acquisition

For the analysis of the generated sarcomere kinetics, as well as the calcium cycling, ionWizard 7.2.2.131 (ionOptix, Westwood/USA) was used. The curve of 10 consecutive contractions was used to calculate the average. (*see Figure 14*) This averaged trace can then be used to calculate the different parameters. Therefore, a curve is fitted automatically to the graph, from which the different variables can be derived. They were transferred into an Excel file, which was then used to make the statistical analysis.

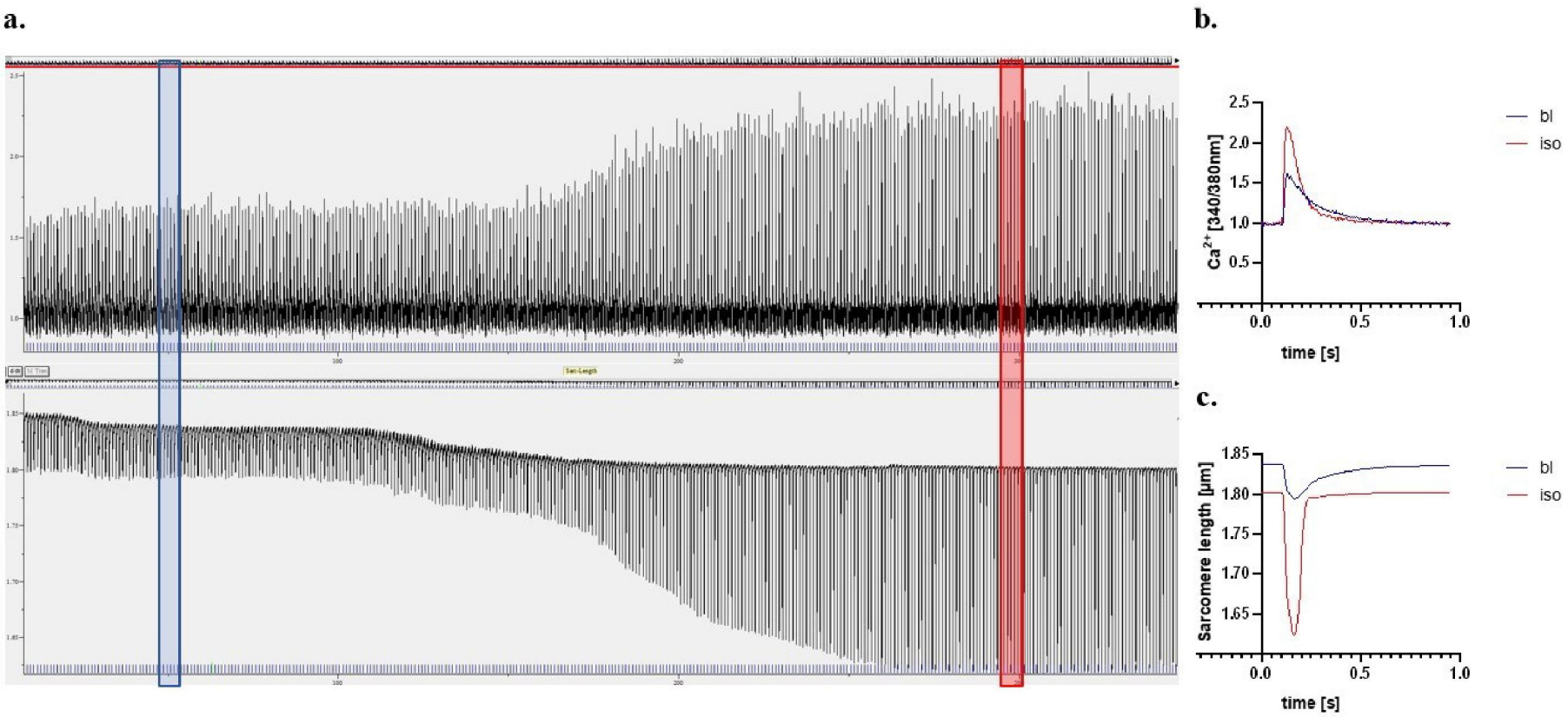

Figure 14 Calcium transients and Sarcomere kinetics of one cardiomyocyte.
a. The illustration shows the resulting trace of a measurement cycle, as plotted by ionWizard. (for further information *see chapter 2.2.3*) The top curve represents the Fura-ratio [340/380], while the bottom curve illustrates the sarcomere length. Highlighted areas show the periods, which were used to average the signal; **b.** and **c.** show the resulting trace with: **b.** Fura ratio and **c.** sarcomere length.
[**blue**… baseline trace (bl), **red**…Isoproterenol stimulated trace (iso)]

2.2.4.2 Statistical analysis

The parameters derived from the measurements of the cells of one isolation were transferred to a Microsoft Excel 365 (Microsoft 365, Redmond/USA) worksheet. There the results were checked for consistency and for data cleansing. After the completion of all measurements, the subset of parameters deemed to be necessary to answer the scientific question, was copied into a separate worksheet, in which the descriptive statistics were generated. It was decided to calculate the median, mean, and standard deviation of the mean for the whole sample as such, as well as for each animal. Due to the nature of the measurements as technical replicates, it was decided that the resulting means of each day should be used as sample for further statistical analysis.

For the analysis and plotting of the data GraphPad Prism 8.0.1 (244) (GraphPad Software, San Diego/USA) was used.

As described above (*see chapter 1.4,* Aim and hypothesis) we hypothesized that Vorinostat's previously described effects were explainable with alterations of the CM's calcium homeostasis. Therefore, we expected the cells of the treated group to show a faster decay of the calcium transient and subsequently a faster relaxation of the cell. Furthermore, due to the faster reuptake, we expected the diastolic calcium levels to be decreased, which in turn should also be reflected in a larger diastolic sarcomere length.

This hypothesis was tested with an unpaired t-test with a level of significance of $\alpha = 0.05$, resulting in a confidence interval of this two-sided test of 95%. The two groups were always tested against each other, when unstimulated, and stimulated with Isoproterenol.

To verify that the required conditions to perform the unpaired t-test were met, the sample was first checked for outliers using the ROUT-test with a maximum false discovery rate Q of 1%. Next the samples were tested to see if they met the characteristics of a Gaussian distribution using the Shapiro-Wilk and Kolmogorov-Smirnov test with a level of significance of $\alpha = 0.05$. Using the Levene's test, the samples were checked for quality of variances.

When the samples were nonparametric, the significance level was tested using the Mann Whitney test. For those with a variance inequality, the unpaired t-test with Welch's correction was used. The nonparametric samples on which one of the two above mentioned tests was performed, are described below. All other comparisons passed the requirements of the unpaired t-test.

Due to the non-Gaussian distribution of the parameters *"time to baseline 50%"* of the sarcomere length before the introduction of Isoproterenol, (*see Figure 17 b.*) as well as

the *"diastolic sarcomere length"* after the Introduction of Isoproterenol (*Figure 15 a.*), the calculation of the significance level was conducted using the Mann-Whitney test.

The variance of the *"calcium return velocity"* of vehicle and verum treated CM before the introduction of Isoproterenol (*see Figure 17 f.*) as well as the *"systolic calcium level"* of vehicle and verum treated CM before the introduction of Isoproterenol (*Figure 15 d.*) were significantly different, therefore the unpaired t test with Welch correction was calculated.

All parameters were then plotted as column bar charts, displaying the means and the standard deviation. The five means for each animal are displayed in each graphic with a small plus-sign in the corresponding graph.

3 Results

As already described above, (*1.4, Aim and hypothesis*) the aim of this study was to assess the contractility of murine CM by means of sarcomere shortening against the calcium transients, measured with the Ca^{2+} sensitive dye Fura-2 AM. For this purpose, we compared 2 groups: verum treated (*DMSO 0.1% + Vorinostat 5µM for 90'*) vs. vehicle treated (*DMSO 0.1% for 90'*) cardiomyocytes. Sarcomere kinetics and calcium flux were analysed at two points in time, before as well as after the introduction of Isoproterenol.

3.1 Baseline characteristics

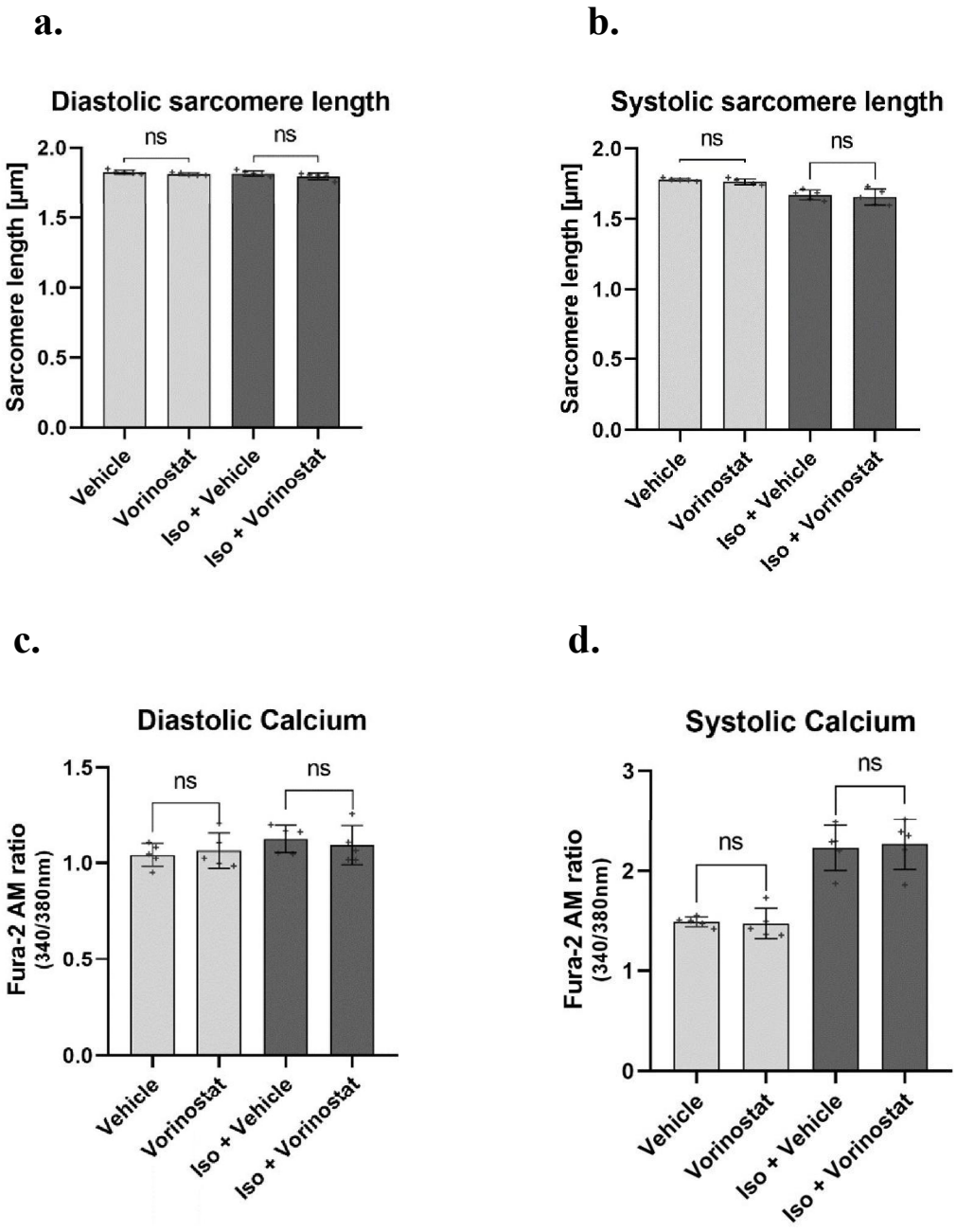

Figure 15 Baseline-characteristics of the cardiomyocyte during systole and diastole

Ad Figure 15: The two groups did not differ in sarcomere length (**a.** and **b.**) or calcium signal (**c.** and **d.**); **a.** Maximal diastolic sarcomere length, **b.** Minimal systolic sarcomere length, **c.** Minimal diastolic calcium signal, **d.** Maximal systolic calcium signal
Sarcomere length in µm, calcium signal as ratio between the Fura-2 AM 340nm and 380nm signals, n_{mouse}= 5 | n_{cells}= 28-32

In the four graphs the main baseline characteristics of the single-cell cardiomyocytes, the minimal length of the sarcomere during the systole and the maximum length during the diastole, as well as the corresponding calcium transients as the ratio of Fura (340/380) are plotted. The baseline parameters showed comparable characteristics in the two groups. Neither before, nor after the introduction of Isoproterenol, the difference reached a level of significance.

The corresponding descriptive statistics to the graphs are collected in *Table 13*.

	Vehicle	**Vorinostat**	**Iso + Vehicle**	**Iso + Vorinostat**
n	5	5	5	5
Diastolic sarcomere length				
Minimum	1.811	1.804	1.794	1.757
Maximum	1.85	1.825	1.845	1.815
Range	0.039	0.021	0.051	0.058
Mean	1.827	1.813	1.818	1.797
STD	0.01447	0.009985	0.01899	0.02309
SEM	0.00647	0.004465	0.008495	0.01033
Systolic sarcomere length				
Minimum	1.767	1.742	1.627	1.597
Maximum	1.795	1.795	1.716	1.733
Range	0.028	0.053	0.089	0.136
Mean	1.78	1.765	1.673	1.657
STD	0.01004	0.02123	0.03566	0.05793
SEM	0.00449	0.009494	0.01595	0.02591
Diastolic calcium				
Minimum	0.95	0.984	1.046	1.014
Maximum	1.105	1.203	1.197	1.259
Range	0.155	0.219	0.151	0.245
Mean	1.041	1.063	1.123	1.092
STD	0.0597	0.09121	0.07059	0.101
SEM	0.0267	0.04079	0.03157	0.04517
Systolic calcium				
Minimum	1.425	1.364	1.873	1.862
Maximum	1.557	1.733	2.488	2.519
Range	0.132	0.369	0.615	0.657
Mean	1.496	1.48	2.229	2.266
STD	0.04858	0.152	0.225	0.2508
SEM	0.02173	0.06797	0.1006	0.1122

Table 13 Descriptive statistics of the baseline-characteristics of the cardiomyocyte
Iso… Isoproterenol, STD… Standard deviation, SEM… Standard Error of the mean

3.2 Systolic hallmarks

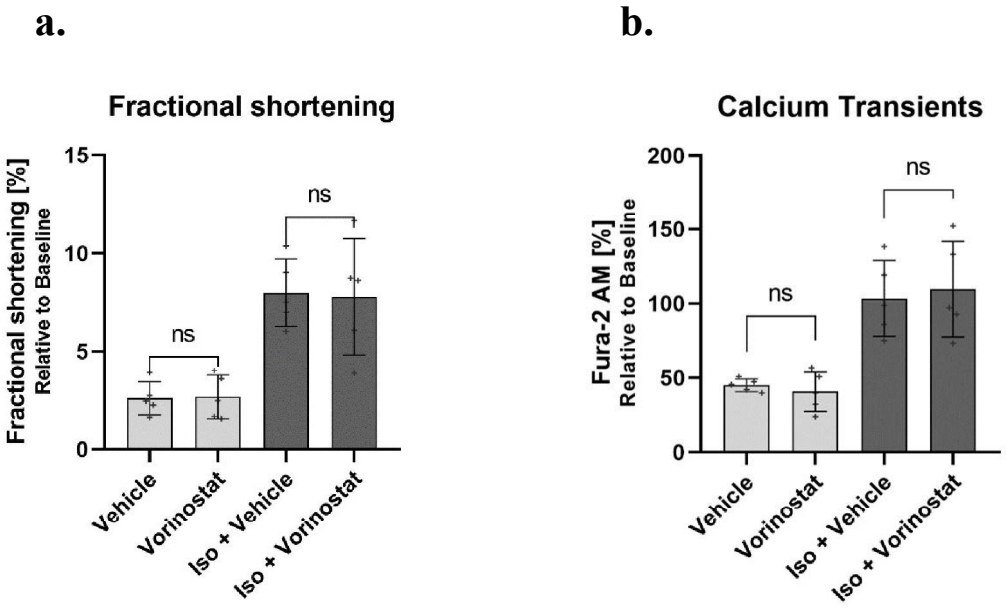

Figure 16 Systolic hallmark features of single-cell cardiomyocytes
Treatment with Vorinostat did not alter the cells systolic function, displayed by the corresponding hallmark features of single-cell cardiomyocytes fractional shortening (**a**.) and peak calcium transient (**b**.); **a.** Maximal systolic contraction, **b.** Peak systolic Fura-2 AM ratio (340/380nm) signal
Parameters displayed in [%] relative to the diastolic (Baseline) signal, n_{mouse}= 5 | n_{cells}= 28-32

The two graphs show the systolic signals relative to the baseline (diastolic) length respectively the fluorescence signal. These parameters reduce the impact of confounders, as for example, cell to cell variation in length due to the isolation or signal processing alterations in the software. The higher the percentage in the fractional shortening, the higher is the cell's ability to contract, indicating a better systolic function. Since calcium is required for the contraction, it is also one of the key drivers of contractility. Thus, a higher signal would be consistent with a better contractile function.

Both the cells in the treatment and the vehicle group showed similar contractile properties (*Figure 16, a*). Likewise, the peak calcium transient was only insignificantly different when incubated with or without Vorinostat (*Figure 16, b*). The same was true if Isoproterenol was introduced into the perfusion chamber. The difference neither in the sarcomere shortening, nor the calcium signal reached a level of significance.

The corresponding descriptive statistics of the graphs in *Figure 16* are collected in *Table 14*.

	Vehicle	*Vorinostat*	*Iso + Vehicle*	*Iso + Vorinostat*
n	*5*	*5*	*5*	*5*
Fractional shortening				
Minimum	*1.615*	*1.541*	*6.035*	*3.858*
Maximum	*3.885*	*4.011*	*10.39*	*11.68*
Range	*2.27*	*2.47*	*4.351*	*7.826*
Mean	*2.582*	*2.652*	*7.997*	*7.797*
STD	*0.8354*	*1.114*	*1.719*	*2.964*
SEM	*0.3736*	*0.4982*	*0.7687*	*1.325*
calcium transient				
Minimum	*39.86*	*23.84*	*75.02*	*73.29*
Maximum	*50.85*	*56.64*	*138.3*	*152.1*
Range	*10.99*	*32.8*	*63.27*	*78.84*
Mean	*45.16*	*40.72*	*103.4*	*109.7*
STD	*4.331*	*13.33*	*25.5*	*32.09*
SEM	*1.937*	*5.962*	*11.41*	*14.35*

Table 14 Descriptive statistics of hallmarks of the systolic function of single-cell cardiomyocytes
Iso… Isoproterenol, STD… Standard deviation, SEM… Standard Error of the mean

3.3 Diastolic hallmarks

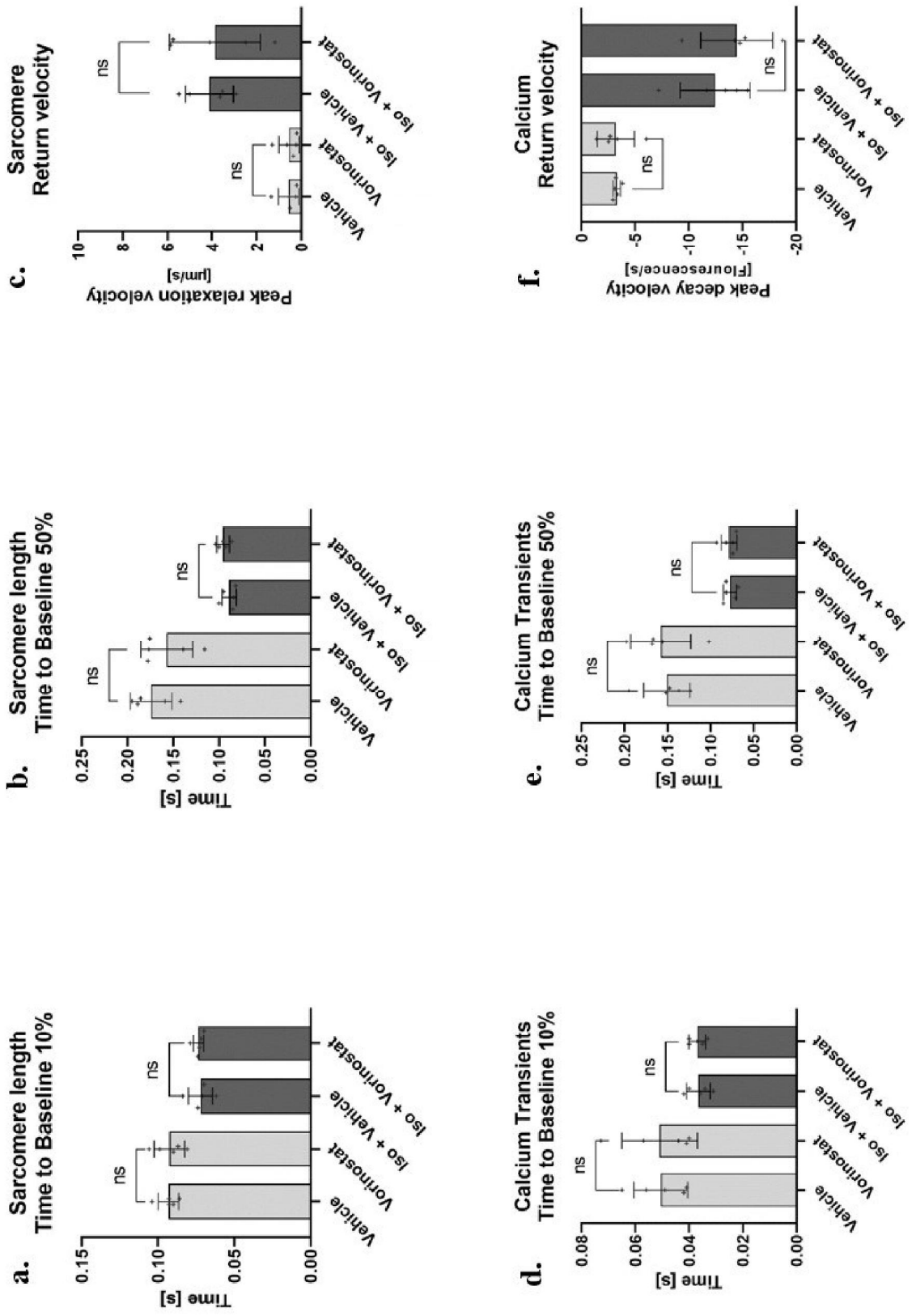

Figure 17 Diastolic hallmark features of single-cell cardiomyocytes

Ad Figure 17: Plotted are hallmark features of the diastolic function respectively their comparable parameters of a single-cell CM. The treatment and vehicle groups did not differ in relaxation times duration (**a.** and **b.**) or speed (**c.**). The corresponding calcium signals decay times (**d.** and **e.**) and speed (**f**.) were in both groups similar as well; **a.** Duration to reach 10% relaxation (difference of diastolic and systolic sarcomere lengths), **b.** Duration to reach 50% relaxation (difference of diastolic and systolic sarcomere lengths), **c.** Maximal sarcomere relaxation velocity, **d.** Duration to reach 10% decay (difference of diastolic and systolic Fura ratio signal), **e.** Duration to reach 50% decay (difference of diastolic and systolic Fura ratio signal), **f.** Maximal decay velocity of the calcium signal (Fura ratio)
Sarcomere length in µm, calcium signal as ratio between the Fura-2 AM 340nm and 380nm signals, n_{mouse}= 5 | n_{cells}= 28-32

The graphs plotted in Figure 17 show the corresponding hallmarks of single-cell cardiomyocytes of the diastolic function of the heart.

In the case of the sarcomere length, a shorter time interval to reach 10% or 50% of relaxation indicates a faster relaxation. The treated and the untreated cells behaved similarly regarding their relaxation both in the early (*Figure 17, a.*), as well as the late phase (*Figure 17, b.*). After the introduction of Isoproterenol, the positive lusitropic effect of the drug could be detected, but other than that, no difference was seen between Vorinostat or vehicle. There was also no change in the peak relaxation velocity (*Figure 17, c.*).

As calcium is one key player of the contractile apparatus of the cardiac muscle (therefore also affecting relaxation), the results of the Fura ratio complete the picture. (*see chapter 1.5.1, Excitation contraction coupling*) No significant difference was detected in the early (*Figure 17, d.*), as well as the late decay (*Figure 17, e.*) of the calcium level. A lower time to reach a clearing of 10% or 50% of the systolic calcium level allows for a faster relaxation and is therefore a surrogate parameter for a better diastolic function. As Isoproterenol induces SERCA activity, the calcium clearing occurred faster after the introduction of the drug, (*cf. 2.2.3.2.1 Isoproterenol*) but there were insignificant differences between the Vorinostat respectively the vehicle groups. In accordance with the results, the maximal calcium clearing rate (*Figure 17, f.*) was faster in the Isoproterenol stimulated cells, but other than that only insignificantly different.

The descriptive statistics about the graphs plotted in *Figure 17* are collected in *Table 15*.

	Vehicle	Vorinostat	Iso + Vehicle	Iso + Vorinostat
n	5	5	5	5
Sarcomere length time to baseline 10%				
Minimum	0.086	0.081	0.062	0.07
Maximum	0.104	0.106	0.084	0.079
Range	0.018	0.025	0.022	0.009
Mean	0.0932	0.0926	0.0722	0.0736
STD	0.006686	0.009915	0.00795	0.003362
SEM	0.00299	0.004434	0.003555	0.001503
Sarcomere length time to baseline 50%				
Minimum	0.142	0.116	0.082	0.086
Maximum	0.195	0.178	0.1	0.104
Range	0.053	0.062	0.018	0.018
Mean	0.1742	0.1572	0.0892	0.0958
STD	0.02269	0.02831	0.007855	0.00687
SEM	0.01015	0.01266	0.003513	0.003072
Sarcomere length peak return velocity				
Minimum	0.217	0.213	2.936	1.186
Maximum	1.363	1.314	5.498	5.859
Range	1.146	1.101	2.562	4.673
Mean	0.5796	0.5592	4.129	3.883
STD	0.4615	0.4573	1.078	2.039
SEM	0.2064	0.2045	0.4821	0.9118
Calcium Transients time to baseline 10%				
Minimum	0.041	0.04	0.031	0.033
Maximum	0.065	0.073	0.042	0.04
Range	0.024	0.033	0.011	0.007
Mean	0.0506	0.051	0.0366	0.037
STD	0.01006	0.01405	0.00445	0.003082
SEM	0.004501	0.006285	0.00199	0.001378
Calcium Transients time to baseline 50%				
Minimum	0.124	0.102	0.068	0.07
Maximum	0.195	0.198	0.085	0.093
Range	0.071	0.096	0.017	0.023
Mean	0.1512	0.1582	0.0776	0.0786
STD	0.02679	0.03507	0.00757	0.009154
SEM	0.01198	0.01569	0.003385	0.004094
Calcium Transients peak decay velocity				
Minimum	-3.828	-6.031	-15.5	-18.74
Maximum	-2.929	-1.379	-7.191	-9.356
Range	0.8995	4.653	8.306	9.381
Mean	-3.273	-3.181	-12.45	-14.47
STD	0.3454	1.74	3.262	3.357
SEM	0.1545	0.7782	1.459	1.501

Table 15 Descriptive statistics of hallmarks of the diastolic function of single-cell cardiomyocytes
Iso… Isoproterenol, STD… Standard deviation, SEM… Standard Error of the mean

4 Discussion

In recent literature there is considerable evidence showing beneficial effects, which are elicited by HDACi such as Vorinostat or Givinostat in animal models on the progression of HF. In different studies (101,109–111,113,130) treatment leads to an improved diastolic and systolic cardiac function, as well as surrogate parameters of clinical improvement. (*for more details see chapter 1.3.7, HDACi treatment and HF*) However, the exact mechanism causing the seen effects remains poorly understood. As calcium is the key ion in the cardiomyocyte's excitation-contraction-coupling (ECC), we suspected its involvement in the drug's mechanism of action. Therefore, we hypothesized that compared to vehicle treated cells, the incubation of murine CM with Vorinostat results in (*i*) a faster relaxation of the cell due to (*ii*) increased calcium clearance out of the cell's cytosol. (*for more details see chapter 1.4, Aim and hypothesis*)

4.1.1 Sarcomere kinetics

With the measurements we conducted, we were not able to detect any significant effect of Vorinostat on both, the contraction as well as calcium concentrations and the relaxation kinetics of murine cardiomyocytes. Neither the examined diastolic nor the systolic hallmark features of cardiomyocytes were affected significantly by Vorinostat. These findings are consistent, both at baseline, as well as when stimulated with Isoproterenol.

Therefore, we cannot confirm our hypothesis, that acute treatment with Vorinostat in murine CM leads to an improved relaxation of the cell.

4.1.2 Calcium cycling

With the measured calcium kinetics we were not able to pick up a difference in the flux of said ion induced by the incubation with Vorinostat. These findings are consistent, both at baseline and when the cells were stimulated with the beta-adrenergic drug Isoproterenol.

Therefore, our second hypothesis is rebutted. We could not confirm the involvement of calcium clearance in the mechanism of action of Vorinostat.

Yet the fact that Sarcomere shortening respectively relaxation were unaffected by the treatment riases further questions. This finding questions Vorinostat's effect on single-cell CM derived from a healthy mouse.

4.2 Hyperacute effects protocol

We initially planned on conducting two sets of experiments. In addition to the present (preincubation) protocol, we tried to investigate the hyperacute effects of Vorinostat on murine CM. For this we wanted to use the whole incubation time of 90' to measure cardiomyocytes whilst incubating them with Isoproterenol and Vorinostat. We discontinued this approach for various reasons. Firstly, the cell's adhesion to the glass plate turned out to be inadequate for the long measurement duration. Subsequently the focus of the sarcomere shifted and moved out of plane. This caused the recorded signal to be full of artifacts and thus not adequate for analysis. Other cells completely lost the contact to the glass plate, causing them to float off. Another issue, with the long measurement protocol, was that it took long to characterise the required number of CM to get statistically robust results. Both aspects led to an inadequate number of traces to be fit for analysis. This was the reason that the protocol was discontinued in favour of the second – preincubation – protocol. We decided to repeat the hyperacute experiments only in the presence of promising results using the preincubation strategy.

4.3 Interpretation and limitations

As described above, Wallner et al. (113) reported in an in-vivo model resembling a HFpEF phenotype, positive lusitropic as well as positive inotropic effects, with a chronic treatment with Vorinostat. We suspected alterations in the calcium homeostasis as reason for the seen effects. With our measurements we were not able to detect any significant effect of Vorinostat on healthy murine CM.

Trying to explain the apparent dichotomy between published results and our measurements we came up with several possible explanations, though we have not been able to prove any so far.

4.3.1 Species dependent difference in

In our experiments we used other animal models than previously reported. A difference in species naturally entails a variety of changes to physiologic processes. These range from macroscopic changes, such as anatomy or varying vital parameters, e.g., heart rate or blood pressure, to microscopic changes, such as another protein composition of the contractile apparatus of the cell.

4.3.1.1 Ca^{2+}pumps

For a cell to relax, calcium must be removed from the cytoplasm. As described in chapter 1.5.1 (*Excitation contraction coupling*), this process relies on various ion

transporters and channels, mainly on the SR Ca^{2+}-ATPase pump (*SERCA*) and the Na^{+}/Ca^{2+} exchanger (*NCX*), to a lesser extent on the plasma membrane Ca2+-ATPase (*PMCA*) and the mitochondrial Ca^{2+} uniporter. The ratio of each route on the clearing of calcium differs largely between animals. In rabbits for example, the lion's share of this ion is removed from the cytoplasm by the two enzymes SERCA (~ 70%) and NCX (~28%), whereas this number changes in a rat's CM to roughly ~90% for SERCA and ~7% to NCX. Larger mammals, such as humans, rather match the Ca^{2+}fluxes of a rabbit, whereas smaller ones, like mice behave similarly to a rat. (131,132) Therefore any process which affects any of the named transporters may be detected in the derived cells or not, depending on the quantitative share. Meraviglia et al. (101) was able to attribute parts of Vorinostat's effects on rats to alterations in the Ca^{2+}- handling through the hyperacetylated protein SERCA2a. Treatment leads to an increased activity of the proteins ATPase and as a result higher Ca^{2+} clearing rates. In a second publication (130) the same research group hypothesized about another mode of Vorinostat's action in a diabetic animal model. Treatment resulted in a reduced accumulation of ROS in the diseased (streptozotocin treated) rats.

4.3.1.2 MyHC

Besides these already known effects, Jeong et al. (111) attributed parts of Givinostat's effect to a (novel) nongenomic mechanism of action, involving the heart's myofibrils. (*see chapter 1.3.7 and 4.3.2.1*) It is known that the composition of myofibrils, especially the myosin heavy chain (MyHC), is subject to a huge variability between the species. In mice the alpha-MyHC is more abundant, whereas in large mammals, such as rabbits, cats or pigs, the beta-MyHC can be predominantly found. This leads to variations of the Myosin mobility. Rats exhibit the highest Myosin mobility, followed by mice and then larger animal. (133,134) This very change in the MyHC predominant isoform is one of the reported findings and suspected mechanisms of action of another HDACi, TSA, in a mouse model with thoracic aortic banding. (135) (*see chapter 4.3.2.1, Changes to MyHC*)

4.3.1.3 Titin

Another explanation in line with the finding is the varying composition of Titin in rodents, when compared to larger animals. As previously described Titin is one of the key determinants of diastolic tension in cardiomyocytes. (*see chapter 1.3.2.4.1*) Titin in rodents has a higher content of the N2B isoform, which makes it stiffer when compared to human or other large mammals, which contain more N2BA. The higher restoring forces are needed to sustain the higher heart rates seen in the rodents. (55) Therefore, it is reasonable to assume

that any change to the protein's composition due to a drug's mechanism of action would also be highly dependent on the exact species used.

4.3.2 Healthy vs. diseased animals

As delineated above, the pathophysiology of HFpEF is highly complex (*see chapter 1.3.2*) and is only partly understood until today. Several changes are known to happen to the diseased myocardium (*see above*), one of which are changes to the MyHC. Therefore, any experiment with healthy animals may yield no results, due to the different (patho-) physiology.

4.3.2.1 Changes to MyHC

A different predominant myosin heavy chain isoform may also be elicited by varying chronic diseases, such as pressure overload or changes in the thyroid hormones.(133,135) Hypertrophy of the heart leads to a higher expression of the fetal β-MyHC in mice, when compared to the adult form α-MyHC, which is referred to as *"fetal gene reprogramming"*. Kong et al. (135) were able to reverse this isoform switch in a murine model of trans aortic banding, if the animals were treated with the HDACi Trichostatin A (TSA). This treatment resulted in a higher abundance of α-MyHC. The authors reported, that treatment led to a better LV performance and blunted the otherwise seen hypertrophy, which they attributed at least partially to the favourable properties of α-MyHC. (135)

4.3.2.2 Calcium kinetics

Calcium kinetics are key, both for the contraction and relaxation of a CM and are known to be altered in HFpEF patients. Runte et al. (136) could show in a study, using human myocardial samples, that this is one of the maladaptive changes seen in patients suffering from HFpEF, but not hypertensive heart disease (HHD). The diastolic calcium concentration in diseased patients' cells increased significantly, especially at higher heart rates. This resulted in a slower calcium release during the systole, an incomplete relaxation of the cardiomyocyte and a higher diastolic resting tension.

The importance of both, the animal model, and the disease is underlined in two papers authored by Meraviglia et al. (101) and Bocchi et al. (130). The research group investigated Vorinostat's effect on the calcium handling in healthy (101) as well as diseased (130) rats. The authors could find significant alterations to the flux of the ion, caused by the treatment with Vorinostat, though the significance and translational potential to other species as well as larger animals remains controversial.

Since we characterized Vorinostat's effect in healthy murine CM with our measurements there is no immediate contradiction to the findings in diseased feline CM described by Wallner et al.(113) and other authors. (101,130)

4.3.3 Limitations to the protocol

Numerous measures were taken to avoid any wrongful conclusion based on unreliable measurement results. However, there is always the possibility for systematic error to occur, especially in a complex multidimensional system as the one used.

4.3.3.1 Cell dependent factors

Cell isolation. As already delineated above, the isolation of CM can be challenging and may be prone to problems. Therefore, we adapted the digestion to the changed setup and proved the new protocol due to consistently high-quality cell isolations with appropriate yields using several training animals. Furthermore, since the cells were compared to themselves, isolation variability is highly unlikely to affect the result negatively. Lastly, any impact due to "aging" was accommodated, measuring the cells alternatingly.

Incubation. One problem with Vorinostat is its low solubility in water. Previously we noticed that if Vorinostat was stored in a hydrous solution as aliquots, precipitation may occur on thawing respectively when diluted to make the final concentration. To avoid any systematic error with the measurements with respect to a faulty incubation, special care was given to the detection of flocculation in the solutions, and the protocol was adapted. Vorinostat was therefore dissolved and stored in pure DMSO. With this change no precipitation could be detected on visual inspection, making such a systematic error highly unlikely.

DMSO. One further possible issue may come with the use of DMSO itself as solvent, as it may exert an effect on the cardiomyocytes. We did not conduct a direct comparison of CM with and without the presence of DMSO in the perfusion solution during this set of experiments. However, our own and other research groups had previously shown that a concentration of 0.1 vol.-% does not lead to a measurable effect on the sarcomere shortening, or the calcium handling of a CM. Furthermore DMSO is known to exhibit some HDAC inhibiting properties itself. (93) However, the concentration used in the experiments was magnitudes higher and Vorinostat has significantly higher inhibitory constants. Therefore, we deem the importance of both findings to be low and thus highly unlikely to be

contributing to the seen absence of an effect. Furthermore, Vorinostat's properties had previously been described by other authors using similar protocols. (113)

Dosage. We acknowledge, that best practice recommendations would advise for a dose-response curve, which we deemed too early for the stage of the experiments and therefore not feasible. Instead, we referred to the literature for concentrations as well as incubation times. According to available evidence, we deemed a dose of 5 μM and an incubation time of 90' to be highly sufficient to exhibit the drug's desired effects. (for more *see chapter 1.3.6.2.4, Approved HDAC Inhibitors on the market – Dosage and Incubation time*)

Other possible confounders were already described in chapter 2, "*Material and methods*".

4.3.3.2 Measurement and data acquisition

The conducted measurements seem to be of high quality. Special care was taken to avoid any impact of confounders. Amongst other precautions the temperature of the microscope's perfusion bath was regularly checked and the buffer was warmed accordingly. All light sources in the measurement room were turned off to (i) avoid bleaching and (ii) reduce the background noise. The data analysis was performed according to the manufacturer's recommendation and in a semi blinded fashion. The resulting two independently determined measurands ("*Sarcomere length*" and "*Calcium concentration*" as Fura ratio 340/380) respectively their derived parameters, show consistent behaviour across all measurements. Furthermore, the measured behaviour is consistent with the results in the available literature.

Due to the continuously reasonable quality of the isolations, the thoroughly monitored incubation in accordance with experimental protocols of other and our own research groups as well as the consistency of the measurement results, the findings need to be regarded as reliable.

4.3.3.3 Statistical analysis

One further reason, why we were not able to detect any significant difference between the verum/vehicle groups may be explainable with the sample size. We used a total of 29-32 cells of 5 different animals. From experience in our research group, we know that this number is sufficient to detect strong signals but may be inadequate to detect subtle changes to the sarcomere shortening or the calcium homeostasis. This may be especially

true in the context of an isolation dependent variability as seen with primary mouse cardiomyocytes.

4.4 Conclusions

These findings suggest that (*i*) Vorinostat's acute effects in murine CM are less likely to be explained with a change to the calcium flux. Alternative mechanisms of action of the panHDACi Givinostat have already been described by Jeong et al.(111) (*see chapter 1.3.7 and 4.3*).

Since we could not detect any alterations to the calcium flux, we see our results as further underlining the involvement of the myofilaments, possibly in combination with an alteration of the calcium sensitivity of the protein. However, we were not able to prove any of the conjectures.

Considering recent evidence, this may be deemed a converse result. However, as stated above, previous experiments differed significantly and are therefore not directly comparable to our findings. Most of publications used the results of in-vivo experiments in the context of a chronic treatment. This may give room for various drug targets, eliciting genomic-, metabolic- and other non-cardiac effects. Other notable differences between previously published protocols and ours include the exact drug used, the route of administration, the model organisms and the model of disease.

(ii) We could further provide proof that short-term application of Vorinostat does not exhibit negative cardiac effects over the course of a short-term exposure in adult murine cardiomyocytes. Vorinostat did, when compared to vehicle treated cells, attenuate neither the Sarcomere shortening or relaxation, nor the calcium flux significantly.

In summary, it can be concluded that recent publications presented promising evidence for a positive effect on the progression of HFpEF, elicited by the treatment with Vorinostat. However, due to the complex mechanism of action, as well as the relatively unselective binding characteristics of the drug, the exact reason for the beneficial effects of the drug remain unknown. Therefore, further experiments need to be conducted to investigate the causal effects of non-calcium-based mechanisms. Furthermore, new animal models need to be developed, which mimic the phenotype of the disease seen in human patients more accurately.

Bibliography

1. Statistik Austria. Berichtsjahr nach Gestorbene [Internet]. [cited 2020 Apr 24]. Available from: https://statcube.at/statistik.at/ext/statcube/jsf/tableView/tableView.xhtml

2. Statistik Austria. Berichtsjahr nach Todesursachen gruppiert [Internet]. [cited 2020 Apr 24]. Available from: https://statcube.at/statistik.at/ext/statcube/jsf/tableView/tableView.xhtml

3. Ponikowski P, Voors AA, Anker SD, Bueno H, Cleland JGF, Coats AJS, et al. 2016 ESC Guidelines for the diagnosis and treatment of acute and chronic heart failureThe Task Force for the diagnosis and treatment of acute and chronic heart failure of the European Society of Cardiology (ESC)Developed with the special contribution of the Heart Failure Association (HFA) of the ESC. Eur Heart J. 2016 Jul 14;37(27):2129–200.

4. Zile Michael R., Brutsaert Dirk L. New Concepts in Diastolic Dysfunction and Diastolic Heart Failure: Part I. Circulation. 2002 Mar 19;105(11):1387–93.

5. Kasper DL, Fauci AS, Hauser SL, Longo DL, Jameson JL, Loscalzo J. Harrison's Principles of Internal Medicine 19/E. 19th ed. McGraw-Hill Education / Medical; 2015. 2770 p.

6. Moradi M, Daneshi F, Behzadmehr R, Rafiemanesh H, Bouya S, Raeisi M. Quality of life of chronic heart failure patients: a systematic review and meta-analysis. Heart Fail Rev [Internet]. 2019 Nov 19 [cited 2020 Apr 26]; Available from: https://doi.org/10.1007/s10741-019-09890-2

7. Voigt J, John MS, Taylor A, Krucoff M, Reynolds MR, Gibson CM. A Reevaluation of the Costs of Heart Failure and Its Implications for Allocation of Health Resources in the United States. Clin Cardiol. 2014;37(5):312–21.

8. Dunlay SM, Roger VL, Weston SA, Jiang R, Redfield MM. Longitudinal changes in ejection fraction in heart failure patients with preserved and reduced ejection fraction. Circ Heart Fail. 2012 Nov;5(6):720–6.

9. Cikes M, Solomon SD. Beyond ejection fraction: an integrative approach for assessment of cardiac structure and function in heart failure. Eur Heart J. 2016 Jun 1;37(21):1642–50.

10. Lourenço AP, Leite-Moreira AF, Balligand J-L, Bauersachs J, Dawson D, Boer RA de, et al. An integrative translational approach to study heart failure with preserved ejection fraction: a position paper from the Working Group on Myocardial Function of the European Society of Cardiology. Eur J Heart Fail. 2018;20(2):216–27.

11. Robotham JL, Takata M, Berman M, Harasawa Y. Ejection fraction revisited. Anesthesiol J Am Soc Anesthesiol. 1991;74(1):172–83.

12. Kraigher-Krainer E, Shah AM, Gupta DK, Santos A, Claggett B, Pieske B, et al. Impaired Systolic Function by Strain Imaging in Heart Failure With Preserved Ejection Fraction. J Am Coll Cardiol. 2014 Feb 11;63(5):447–56.

13. Hans-Christian Pape, Armin Kurtz, Stefan Silbernagl. Physiologie. 7th ed. Thieme; 2014.

14. Richard E. Klabunde. CV Physiology | Compliance [Internet]. [cited 2020 Nov 18]. Available from: https://www.cvphysiology.com/Cardiac%20Function/CF013

15. Herold G. Innere Medizin 2014. 1st ed. Köln: Herold, Gerd; 2013. 990 p.

16. Vedin Ola, Lam Carolyn S.P., Koh Angela S., Benson Lina, Teng Tiew Hwa Katherine, Tay Wan Ting, et al. Significance of Ischemic Heart Disease in Patients With Heart Failure and Preserved, Midrange, and Reduced Ejection Fraction. Circ Heart Fail. 2017 Jun 1;10(6):e003875.

17. Lund LH. Heart Failure with Mid-range Ejection Fraction: Lessons from CHARM. Card Fail Rev. 2018 Aug;4(2):70–2.

18. ElGuindy A, Yacoub MH. Heart failure with preserved ejection fraction. Glob Cardiol Sci Pract. 2012 Jul 3;2012(1):10.

19. Ho KK, Pinsky JL, Kannel WB, Levy D. The epidemiology of heart failure: the Framingham Study. J Am Coll Cardiol. 1993 Oct;22(4 Suppl A):6A-13A.

20. Henning RJ. Diagnosis and treatment of heart failure with preserved left ventricular ejection fraction. World J Cardiol. 2020 Jan 26;12(1):7–25.

21. Heidenreich Paul A., Albert Nancy M., Allen Larry A., Bluemke David A., Butler Javed, Fonarow Gregg C., et al. Forecasting the Impact of Heart Failure in the United States. Circ Heart Fail. 2013 May 1;6(3):606–19.

22. Roger Véronique L., Go Alan S., Lloyd-Jones Donald M., Benjamin Emelia J., Berry Jarett D., Borden William B., et al. Heart Disease and Stroke Statistics—2012 Update. Circulation. 2012 Jan 1;125(1):e2–220.

23. Conrad N, Judge A, Tran J, Mohseni H, Hedgecott D, Crespillo AP, et al. Temporal trends and patterns in heart failure incidence: a population-based study of 4 million individuals. Lancet Lond Engl. 2018 10;391(10120):572–80.

24. Bleumink GS, Knetsch AM, Sturkenboom MCJM, Straus SMJM, Hofman A, Deckers JW, et al. Quantifying the heart failure epidemic: prevalence, incidence rate, lifetime risk and prognosis of heart failureThe Rotterdam Study. Eur Heart J. 2004 Sep 1;25(18):1614–9.

25. McDonagh TA, Morrison CE, Lawrence A, Ford I, Tunstall-Pedoe H, McMurray JJ, et al. Symptomatic and asymptomatic left-ventricular systolic dysfunction in an urban population. Lancet Lond Engl. 1997 Sep 20;350(9081):829–33.

26. Ammar KA, Jacobsen SJ, Mahoney DW, Kors JA, Redfield MM, Burnett JC, et al. Prevalence and prognostic significance of heart failure stages: application of the American College of Cardiology/American Heart Association heart failure staging criteria in the community. Circulation. 2007 Mar 27;115(12):1563–70.

27. Owan TE, Redfield MM. Epidemiology of Diastolic Heart Failure. Prog Cardiovasc Dis. 2005 Mar;47(5):320–32.

28. Owan TE, Hodge DO, Herges RM, Jacobsen SJ, Roger VL, Redfield MM. Trends in Prevalence and Outcome of Heart Failure with Preserved Ejection Fraction. http://dx.doi.org/101056/NEJMoa052256. 2006 Jul 20;(355):251–9.

29. Steinberg Benjamin A., Zhao Xin, Heidenreich Paul A., Peterson Eric D., Bhatt Deepak L., Cannon Christopher P., et al. Trends in Patients Hospitalized With Heart Failure and Preserved Left Ventricular Ejection Fraction. Circulation. 2012 Jul 3;126(1):65–75.

30. Shah Kevin S., Xu Haolin, Matsouaka Roland A., Bhatt Deepak L., Heidenreich Paul A., Hernandez Adrian F., et al. Heart Failure With Preserved, Borderline, and Reduced Ejection Fraction: 5-Year Outcomes. J Am Coll Cardiol. 2017 Nov 14;70(20):2476–86.

31. American Cancer Society. Cancer Facts & Figures 2019. 2019;76.

32. Ceia F, Fonseca C, Mota T, Morais H, Matias F, de Sousa A, et al. Prevalence of chronic heart failure in Southwestern Europe: the EPICA study. Eur J Heart Fail. 2002 Aug 1;4(4):531–9.

33. Duca F, Zotter-Tufaro C, Kammerlander AA, Aschauer S, Binder C, Mascherbauer J, et al. Gender-related differences in heart failure with preserved ejection fraction. Sci Rep [Internet]. 2018 Jan 18 [cited 2020 Apr 29];8. Available from: https://www.ncbi.nlm.nih.gov/pmc/articles/PMC5773700/

34. Ho Jennifer E., Enserro Danielle, Brouwers Frank P., Kizer Jorge R., Shah Sanjiv J., Psaty Bruce M., et al. Predicting Heart Failure With Preserved and Reduced Ejection Fraction. Circ Heart Fail. 2016 Jun 1;9(6):e003116.

35. Dunlay SM, Roger VL, Redfield MM. Epidemiology of heart failure with preserved ejection fraction. Nat Rev Cardiol. 2017 Oct;14(10):591–602.

36. Ziaeian B, Fonarow GC. Epidemiology and aetiology of heart failure. Nat Rev Cardiol. 2016 Jun;13(6):368–78.

37. Packer M, Kitzman DW. Obesity-Related Heart Failure With a Preserved Ejection Fraction: The Mechanistic Rationale for Combining Inhibitors of Aldosterone, Neprilysin, and Sodium-Glucose Cotransporter-2. JACC Heart Fail. 2018 Aug;6(8):633–9.

38. Chamberlain AM, St Sauver JL, Gerber Y, Manemann SM, Boyd CM, Dunlay SM, et al. Multimorbidity in heart failure: a community perspective. Am J Med. 2015 Jan;128(1):38–45.

39. Mohammed SF, Hussain S, Mirzoyev SA, Edwards WD, Maleszewski JJ, Redfield MM. Coronary Microvascular Rarefaction and Myocardial Fibrosis in Heart Failure with Preserved Ejection Fraction. Circulation. 2015 Feb 10;131(6):550–9.

40. Fischer M, Baessler A, Hense HW, Hengstenberg C, Muscholl M, Holmer S, et al. Prevalence of left ventricular diastolic dysfunction in the community. Results from a Doppler echocardiographic-based survey of a population sample. Eur Heart J. 2003 Feb;24(4):320–8.

41. Packer Milton, Lam Carolyn S.P., Lund Lars H., Redfield Margaret M. Interdependence of Atrial Fibrillation and Heart Failure With a Preserved Ejection Fraction Reflects a Common Underlying Atrial and Ventricular Myopathy. Circulation. 2020 Jan 7;141(1):4–6.

42. Brouwers FP, de Boer RA, van der Harst P, Voors AA, Gansevoort RT, Bakker SJ, et al. Incidence and epidemiology of new onset heart failure with preserved vs. reduced ejection fraction in a community-based cohort: 11-year follow-up of PREVEND. Eur Heart J. 2013 May 14;34(19):1424–31.

43. Paulus WJ, Tschöpe C. A Novel Paradigm for Heart Failure With Preserved Ejection Fraction: Comorbidities Drive Myocardial Dysfunction and Remodeling Through Coronary Microvascular Endothelial Inflammation. J Am Coll Cardiol. 2013 Jul 23;62(4):263–71.

44. Tam MC, Lee R, Cascino TM, Konerman MC, Hummel SL. Current Perspectives on Systemic Hypertension in Heart Failure with Preserved Ejection Fraction. Curr Hypertens Rep. 2017 Feb;19(2):12.

45. Chamberlain AM, St Sauver JL, Gerber Y, Manemann SM, Boyd CM, Dunlay SM, et al. Multimorbidity in heart failure: a community perspective. Am J Med. 2015 Jan;128(1):38–45.

46. Krüger W. Acute Heart Failure: Putting the Puzzle of Pathophysiology and Evidence Together in Daily Practice. Springer; 2017. 415 p.

47. Glezeva N, Baugh JA. Role of inflammation in the pathogenesis of heart failure with preserved ejection fraction and its potential as a therapeutic target. Heart Fail Rev. 2014 Sep 1;19(5):681–94.

48. Westermann Dirk, Lindner Diana, Kasner Mario, Zietsch Christine, Savvatis K., Escher F., et al. Cardiac Inflammation Contributes to Changes in the Extracellular Matrix in Patients With Heart Failure and Normal Ejection Fraction. Circ Heart Fail. 2011 Jan 1;4(1):44–52.

49. Lam CSP, Brutsaert DL. Endothelial dysfunction: a pathophysiologic factor in heart failure with preserved ejection fraction. J Am Coll Cardiol. 2012 Oct 30;60(18):1787–9.

50. Phan TT, Abozguia K, Nallur Shivu G, Mahadevan G, Ahmed I, Williams L, et al. Heart Failure With Preserved Ejection Fraction Is Characterized by Dynamic Impairment of Active Relaxation and Contraction of the Left Ventricle on Exercise and Associated With Myocardial Energy Deficiency. J Am Coll Cardiol. 2009 Jul 28;54(5):402–9.

51. Penicka M, Vanderheyden M, Bartunek J. Diagnosis of heart failure with preserved ejection fraction: role of clinical Doppler echocardiography. Heart. 2014 Jan 1;100(1):68–76.

52. Mantero A, Gentile F, Gualtierotti C, Azzollini M, Barbier P, Beretta L, et al. Left ventricular diastolic parameters in 288 normal subjects from 20 to 80 years old. Eur Heart J. 1995 Jan;16(1):94–105.

53. Chung Charles S., Hutchinson Kirk R., Methawasin Mei, Saripalli Chandra, Smith John E., Hidalgo Carlos G., et al. Shortening of the Elastic Tandem Immunoglobulin Segment of Titin Leads to Diastolic Dysfunction. Circulation. 2013 Jul 2;128(1):19–28.

54. Granzier HL, Irving TC. Passive tension in cardiac muscle: contribution of collagen, titin, microtubules, and intermediate filaments. Biophys J. 1995 Mar;68(3):1027–44.

55. LeWinter MM, Wu Y, Labeit S, Granzier H. Cardiac titin: Structure, functions and role in disease. Clin Chim Acta. 2007 Jan 1;375(1):1–9.

56. LeWinter MM, Granzier HL. Cardiac Titin and Heart Disease. J Cardiovasc Pharmacol. 2014 Mar;63(3):207–12.

57. Alegre-Cebollada DG Kevin Yan, Carmen L Badilla, Julio M Fernandez & Jorge. Disulfide isomerization reactions in titin immunoglobulin domains enable a mode of protein elasticity [Internet]. 2018 [cited 2021 Jan 27]. Available from: https://commons.wikimedia.org/wiki/File:Titin_IG_Domains.jpg

58. Abudiab MM, Redfield MM, Melenovsky V, Olson TP, Kass DA, Johnson BD, et al. Cardiac output response to exercise in relation to metabolic demand in heart failure with preserved ejection fraction. Eur J Heart Fail. 2013 Jul;15(7):776–85.

59. Roberts E, Ludman AJ, Dworzynski K, Al-Mohammad A, Cowie MR, McMurray JJV, et al. The diagnostic accuracy of the natriuretic peptides in heart failure: systematic review and diagnostic meta-analysis in the acute care setting. The BMJ [Internet]. 2015 Mar 4 [cited 2020 Aug 22];350. Available from: https://www.ncbi.nlm.nih.gov/pmc/articles/PMC4353288/

60. Pieske B, Tschöpe C, de Boer RA, Fraser AG, Anker SD, Donal E, et al. How to diagnose heart failure with preserved ejection fraction: the HFA–PEFF diagnostic algorithm: a consensus recommendation from the Heart Failure Association (HFA) of the European Society of Cardiology (ESC). Eur Heart J. 2019 Oct 21;40(40):3297–317.

61. Ather S, Chan W, Bozkurt B, Aguilar D, Ramasubbu K, Zachariah AA, et al. Impact of noncardiac comorbidities on morbidity and mortality in a predominantly male population with heart failure and preserved versus reduced ejection fraction. J Am Coll Cardiol. 2012 Mar 13;59(11):998–1005.

62. Dorfs S, Zeh W, Hochholzer W, Jander N, Kienzle R-P, Pieske B, et al. Pulmonary capillary wedge pressure during exercise and long-term mortality in patients with suspected heart failure with preserved ejection fraction. Eur Heart J. 2014 Nov 21;35(44):3103–12.

63. Kaye D, Shah SJ, Borlaug BA, Gustafsson F, Komtebedde J, Kubo S, et al. Effects of an Interatrial Shunt on Rest and Exercise Hemodynamics: Results of a Computer Simulation in Heart Failure. J Card Fail. 2014 Mar 1;20(3):212–21.

64. Kaye DM, Nanayakkara S. Interatrial Shunt Device for Heart Failure With Preserved Ejection Fraction. Front Cardiovasc Med [Internet]. 2019 Sep 18 [cited 2020 Jul 29];6. Available from: https://www.ncbi.nlm.nih.gov/pmc/articles/PMC6759808/

65. Kaye David M., Hasenfuß Gerd, Neuzil Petr, Post Martijn C., Doughty Robert, Trochu Jean-Noël, et al. One-Year Outcomes After Transcatheter Insertion of an Interatrial Shunt Device for the Management of Heart Failure With Preserved Ejection Fraction. Circ Heart Fail. 2016 Dec 1;9(12):e003662.

66. Hasenfuß G, Hayward C, Burkhoff D, Silvestry FE, McKenzie S, Gustafsson F, et al. A transcatheter intracardiac shunt device for heart failure with preserved ejection fraction (REDUCE LAP-HF): a multicentre, open-label, single-arm, phase 1 trial. The Lancet. 2016 Mar 26;387(10025):1298–304.

67. Kaye DM, Petrie MC, McKenzie S, Hasenfuβ G, Malek F, Post M, et al. Impact of an interatrial shunt device on survival and heart failure hospitalization in patients with preserved ejection fraction. ESC Heart Fail. 2019;6(1):62–9.

68. Felsenfeld G, Groudine M. Controlling the double helix. Nature. 2003 Jan;421(6921):448–53.

69. Kornberg RD. Chromatin Structure: A Repeating Unit of Histones and DNA. Science. 1974 May 24;184(4139):868–71.

70. Bannister AJ, Kouzarides T. Regulation of chromatin by histone modifications. Cell Res. 2011 Mar;21(3):381–95.

71. Redon C, Pilch D, Rogakou E, Sedelnikova O, Newrock K, Bonner W. Histone H2A variants H2AX and H2AZ. Curr Opin Genet Dev. 2002 Apr 1;12(2):162–9.

72. Martire S, Banaszynski LA. The roles of histone variants in fine-tuning chromatin organization and function. Nat Rev Mol Cell Biol. 2020 Jul 14;1–20.

73. Falkenberg KJ, Johnstone RW. Histone deacetylases and their inhibitors in cancer, neurological diseases and immune disorders. Nat Rev Drug Discov. 2014 Sep;13(9):673–91.

74. Yang X-J, Seto E. HATs and HDACs: from structure, function and regulation to novel strategies for therapy and prevention. Oncogene. 2007 Aug 1;26(37):5310–8.

75. Becker PB, Hörz W. ATP-Dependent Nucleosome Remodeling. Annu Rev Biochem. 2002 Jun 1;71(1):247–73.

76. Ali I, Conrad RJ, Verdin E, Ott M. Lysine Acetylation Goes Global: From Epigenetics to Metabolism and Therapeutics. Chem Rev. 2018 Feb 14;118(3):1216–52.

77. Controlling the double helix | Nature [Internet]. [cited 2020 Jul 30]. Available from: https://www.nature.com/articles/nature01411

78. Weinert BT, Iesmantavicius V, Wagner SA, Schölz C, Gummesson B, Beli P, et al. Acetyl-Phosphate Is a Critical Determinant of Lysine Acetylation in E. coli. Mol Cell. 2013 Jul 25;51(2):265–72.

79. Bagchi RA, Weeks KL. Histone deacetylases in cardiovascular and metabolic diseases. J Mol Cell Cardiol. 2019 May 1;130:151–9.

80. Unraveling the hidden catalytic activity of vertebrate class IIa histone deacetylases | PNAS [Internet]. [cited 2020 Aug 7]. Available from: https://www.pnas.org/content/104/44/17335

81. Fischle W, Dequiedt F, Hendzel MJ, Guenther MG, Lazar MA, Voelter W, et al. Enzymatic Activity Associated with Class II HDACs Is Dependent on a Multiprotein Complex Containing HDAC3 and SMRT/N-CoR. Mol Cell. 2002 Jan 1;9(1):45–57.

82. Guenther MG, Barak O, Lazar MA. The SMRT and N-CoR Corepressors Are Activating Cofactors for Histone Deacetylase 3. Mol Cell Biol. 2001 Sep;21(18):6091–101.

83. Humphrey GW, Wang Y, Russanova VR, Hirai T, Qin J, Nakatani Y, et al. Stable histone deacetylase complexes distinguished by the presence of SANT domain proteins CoREST/kiaa0071 and Mta-L1. J Biol Chem. 2001 Mar 2;276(9):6817–24.

84. Haberland M, Montgomery RL, Olson EN. The many roles of histone deacetylases in development and physiology: implications for disease and therapy. Nat Rev Genet. 2009 Jan;10(1):32–42.

85. McKinsey TA. Therapeutic Potential for HDAC Inhibitors in the Heart. Annu Rev Pharmacol Toxicol. 2012 Jan 11;52(1):303–19.

86. Lu J, McKinsey TA, Nicol RL, Olson EN. Signal-dependent activation of the MEF2 transcription factor by dissociation from histone deacetylases. Proc Natl Acad Sci U S A. 2000 Apr 11;97(8):4070–5.

87. McKinsey TA, Zhang CL, Olson EN. MEF2: a calcium-dependent regulator of cell division, differentiation and death. Trends Biochem Sci. 2002 Jan;27(1):40–7.

88. Antos CL, McKinsey TA, Dreitz M, Hollingsworth LM, Zhang C-L, Schreiber K, et al. Dose-dependent Blockade to Cardiomyocyte Hypertrophy by Histone Deacetylase Inhibitors. J Biol Chem. 2003 Jan 8;278(31):28930–7.

89. Friend C, Scher W, Holland JG, Sato T. Hemoglobin Synthesis in Murine Virus-Induced Leukemic Cells In Vitro: Stimulation of Erythroid Differentiation by Dimethyl Sulfoxide. Proc Natl Acad Sci. 1971 Feb 1;68(2):378–82.

90. Marks PA, Breslow R. Dimethyl sulfoxide to vorinostat: development of this histone deacetylase inhibitor as an anticancer drug. Nat Biotechnol. 2007 Jan;25(1):84–90.

91. Li P, Ge J, Li H. Lysine acetyltransferases and lysine deacetylases as targets for cardiovascular disease. Nat Rev Cardiol. 2020 Feb;17(2):96–115.

92. Gerbeth L, Glauben R. HDAC und HDAC-Inhibition in der klinischen Forschung. [cited 2020 Aug 19];(04/2019). Available from: https://www.trillium.de/zeitschriften/trillium-immunologie/archiv/ausgaben-2019/heft-42019/aus-der-klinischen-forschung/hdac-und-hdac-inhibition-in-der-klinischen-forschung.html

93. Bush Erik W., McKinsey Timothy A. Protein Acetylation in the Cardiorenal Axis. Circ Res. 2010 Feb 5;106(2):272–84.

94. Eckschlager T, Plch J, Stiborova M, Hrabeta J. Histone Deacetylase Inhibitors as Anticancer Drugs. Int J Mol Sci [Internet]. 2017 Jul 1 [cited 2020 Aug 19];18(7). Available from: https://www.ncbi.nlm.nih.gov/pmc/articles/PMC5535906/

95. Skipper PL, Tannenbaum SR, Thilly WG, Furth EE, Bishop WW. Mutagenicity of hydroxamic acids and the probable involvement of carbamoylation. Cancer Res. 1980 Dec;40(12):4704–8.

96. Package insert Zolinza [Internet]. [cited 2020 Aug 19]. Available from: https://www.merck.com/product/usa/pi_circulars/z/zolinza/zolinza_pi.pdf

97. Richon VM. Cancer biology: mechanism of antitumour action of vorinostat (suberoylanilide hydroxamic acid), a novel histone deacetylase inhibitor. Br J Cancer. 2006 Dec;95(1):S2–6.

98. Chou CJ, Herman D, Gottesfeld JM. Pimelic Diphenylamide 106 Is a Slow, Tight-binding Inhibitor of Class I Histone Deacetylases. J Biol Chem. 2008 Dec 19;283(51):35402–9.

99. University College London. Enzyme inhibitors [Internet]. [cited 2020 Aug 21]. Available from: https://www.ucl.ac.uk/~ucbcdab/enzass/inhibition.htm#Ki

100. Tiffon C, Adams J, van der Fits L, Wen S, Townsend P, Ganesan A, et al. The histone deacetylase inhibitors vorinostat and romidepsin downmodulate IL-10 expression in cutaneous T-cell lymphoma cells. Br J Pharmacol. 2011 Apr;162(7):1590–602.

101. Meraviglia V, Bocchi L, Sacchetto R, Florio MC, Motta BM, Corti C, et al. HDAC Inhibition Improves the Sarcoendoplasmic Reticulum Ca2+-ATPase Activity in Cardiac Myocytes. Int J Mol Sci. 2018 Jan 31;19(2).

102. Kerr JS, Galloway S, Lagrutta A, Armstrong M, Miller T, Richon VM, et al. Nonclinical Safety Assessment of the Histone Deacetylase Inhibitor Vorinostat. Int J Toxicol. 2010 Jan 1;29(1):3–19.

103. Miles MA, Harris MA, Hawkins CJ. Proteasome inhibitors trigger mutations via activation of caspases and CAD, but mutagenesis provoked by the HDAC inhibitors vorinostat and romidepsin is caspase/CAD-independent. Apoptosis. 2019 Jun 1;24(5):404–13.

104. Hypoxanthin-Guanin-Phosphoribosyltransferase. In: Wikipedia [Internet]. 2017 [cited 2021 Jan 8]. Available from: https://de.wikipedia.org/w/index.php?title=Hypoxanthin-Guanin-Phosphoribosyltransferase&oldid=168831944

105. Kelly WK, O'Connor OA, Krug LM, Chiao JH, Heaney M, Curley T, et al. Phase I Study of an Oral Histone Deacetylase Inhibitor, Suberoylanilide Hydroxamic Acid, in Patients With Advanced Cancer. J Clin Oncol. 2005 Jun 10;23(17):3923–31.

106. Munster PN, Rubin EH, Belle SV, Friedman E, Patterson JK, Dyck KV, et al. A Single Supratherapeutic Dose of Vorinostat Does Not Prolong the QTc Interval in Patients with Advanced Cancer. Clin Cancer Res. 2009 Nov 15;15(22):7077–84.

107. Lynch DR, Washam JB, Newby LK. QT interval prolongation and torsades de pointes in a patient undergoing treatment with vorinostat: a case report and review of the literature. Cardiol J. 2012;19(4):434–8.

108. hERG. In: Wikipedia [Internet]. 2020 [cited 2021 Jan 15]. Available from: https://en.wikipedia.org/w/index.php?title=HERG&oldid=997376539

109. Xie M, Tang Y, Hill JA. HDAC inhibition as a therapeutic strategy in myocardial ischemia/reperfusion injury. J Mol Cell Cardiol. 2019 Apr;129:188–92.

110. Xie Min, Kong Yongli, Tan Wei, May Herman, Battiprolu Pavan K., Pedrozo Zully, et al. Histone Deacetylase Inhibition Blunts Ischemia/Reperfusion Injury by Inducing Cardiomyocyte Autophagy. Circulation. 2014 Mar 11;129(10):1139–51.

111. Jeong MY, Lin YH, Wennersten SA, Demos-Davies KM, Cavasin MA, Mahaffey JH, et al. Histone deacetylase activity governs diastolic dysfunction through a nongenomic mechanism. Sci Transl Med. 2018 07;10(427).

112. Poggesi C, Tesi C, Stehle R. Sarcomeric determinants of striated muscle relaxation kinetics. Pflugers Arch. 2005 Mar;449(6):505–17.

113. Wallner M, Eaton DM, Berretta RM, Liesinger L, Schittmayer M, Gindlhuber J, et al. HDAC inhibition improves cardiopulmonary function in a feline model of diastolic dysfunction. Sci Transl Med. 2020 Jan 8;12(525).

114. Wallner M, Eaton DM, Berretta RM, Borghetti G, Wu J, Baker ST, et al. A Feline HFpEF Model with Pulmonary Hypertension and Compromised Pulmonary Function. Sci Rep. 2017 Nov 29;7(1):16587.

115. Cardiac excitation-contraction coupling. In: Wikipedia [Internet]. 2019 [cited 2021 Jan 27]. Available from: https://en.wikipedia.org/w/index.php?title=Cardiac_excitation-contraction_coupling&oldid=913715935

116. Eisner David A., Caldwell Jessica L., Kistamás Kornél, Trafford Andrew W. Calcium and Excitation-Contraction Coupling in the Heart. Circ Res. 2017 Jul 7;121(2):181–95.

117. Troponin. In: Wikipedia [Internet]. 2021 [cited 2021 Jan 27]. Available from: https://en.wikipedia.org/w/index.php?title=Troponin&oldid=997694211

118. Louch WE, Sheehan KA, Wolska BM. Methods in cardiomyocyte isolation, culture, and gene transfer. J Mol Cell Cardiol. 2011 Sep;51(3):288–98.

119. Isenberg G, Klockner U. Calcium tolerant ventricular myocytes prepared by preincubation in a “KB medium.” Pflüg Arch. 1982 Oct 1;395(1):6–18.

120. LiberaseTM TM Research Grade Protocol & Troubleshooting [Internet]. Sigma-Aldrich. [cited 2020 Sep 16]. Available from: https://www.sigmaaldrich.com/technical-documents/protocols/biology/roche/liberase-tm-research-grade.html

121. Piper HM. The calcium paradox revisitedAn artefact of great heuristic value. Cardiovasc Res. 2000 Jan 1;45(1):123–7.

122. Abrams DJ, Saffitz JE. Chapter 11 - Diseases of the Intercalated Disc. In: Jefferies JL, Blaxall BC, Robbins J, Towbin JA, editors. Cardioskeletal Myopathies in Children and Young Adults [Internet]. Boston: Academic Press; 2017 [cited 2020 Sep 16]. p. 213–31. Available from: http://www.sciencedirect.com/science/article/pii/B978012800040300011X

123. Niessen CM. Tight Junctions/Adherens Junctions: Basic Structure and Function. J Invest Dermatol. 2007 Nov 1;127(11):2525–32.

124. Ion Optix LLC. HMSYS: Myocyte Calcium & Contractility Recording System [Internet]. [cited 2020 Sep 11]. Available from: http://science.kyst.com.tw/upload/pdfs1207021409159030.pdf

125. Oakes SG, Martin WJ, Lisek CA, Powis G. Incomplete hydrolysis of the calcium indicator precursor fura-2 pentaacetoxymethyl ester (fura-2 AM) by cells. Anal Biochem. 1988 Feb 15;169(1):159–66.

126. Product information Fura and Indo Ratiometric Calcium Indicators [Internet]. [cited 2020 Sep 13]. Available from: https://assets.thermofisher.com/TFS-Assets/LSG/manuals/mp01200.pdf

127. Fura-2-acetoxymethyl ester. In: Wikipedia [Internet]. 2019 [cited 2020 Sep 14]. Available from: https://en.wikipedia.org/w/index.php?title=Fura-2-acetoxymethyl_ester&oldid=919880655

128. Silbernagl S. Taschenatlas Physiologie. 8. Edition. Stuttgart New York: Thieme; 2012. 472 p.

129. L-type calcium channel. In: Wikipedia [Internet]. 2021 [cited 2021 Jan 10]. Available from: https://en.wikipedia.org/w/index.php?title=L-type_calcium_channel&oldid=999078745

130. Bocchi L, Motta BM, Savi M, Vilella R, Meraviglia V, Rizzi F, et al. The Histone Deacetylase Inhibitor Suberoylanilide Hydroxamic Acid (SAHA) Restores Cardiomyocyte Contractility in a Rat Model of Early Diabetes. Int J Mol Sci. 2019 Apr 16;20(8).

131. Bögeholz N, Muszynski A, Pott C. The physiology of cardiac calcium handling. Wien Med Wochenschr. 2012 Jul 1;162(13):278–82.

132. Bers DM. Cardiac excitation–contraction coupling. Nature. 2002 Jan;415(6868):198–205.

133. Lompre AM, Mercadier JJ, Wisnewsky C, Bouveret P, Pantaloni C, D'Albis A, et al. Species- and age-dependent changes in the relative amounts of cardiac myosin isoenzymes in mammals. Dev Biol. 1981 Jun 1;84(2):286–90.

134. Malmqvist UP, Aronshtam A, Lowey S. Cardiac myosin isoforms from different species have unique enzymatic and mechanical properties. Biochemistry. 2004 Nov 30;43(47):15058–65.

135. Kong Yongli, Tannous Paul, Lu Guangrong, Berenji Kambeez, Rothermel Beverly A., Olson Eric N., et al. Suppression of Class I and II Histone Deacetylases Blunts Pressure-Overload Cardiac Hypertrophy. Circulation. 2006 Jun 6;113(22):2579–88.

136. Runte KE, Bell SP, Selby DE, Häußler TN, Ashikaga T, LeWinter MM, et al. Relaxation and the Role of Calcium in Isolated Contracting Myocardium from Patients with Hypertensive Heart Disease and Heart Failure with Preserved Ejection Fraction. Circ Heart Fail [Internet]. 2017 Aug [cited 2020 Nov 20];10(8). Available from: https://www.ncbi.nlm.nih.gov/pmc/articles/PMC5567852/